INFORMATION TO USERS

This manuscript has been reproduced from the microfilm master. UMI films the text directly from the original or copy submitted. Thus, some thesis and dissertation copies are in typewriter face, while others may be from any type of computer printer.

The quality of this reproduction is dependent upon the quality of the copy submitted. Broken or indistinct print, colored or poor quality illustrations and photographs, print bleedthrough, substandard margins, and improper alignment can adversely affect reproduction.

In the unlikely event that the author did not send UMI a complete manuscript and there are missing pages, these will be noted. Also, if unauthorized copyright material had to be removed, a note will indicate the deletion.

Oversize materials (e.g., maps, drawings, charts) are reproduced by sectioning the original, beginning at the upper left-hand corner and continuing from left to right in equal sections with small overlaps. Each original is also photographed in one exposure and is included in reduced form at the back of the book.

Photographs included in the original manuscript have been reproduced xerographically in this copy. Higher quality 6" x 9" black and white photographic prints are available for any photographs or illustrations appearing in this copy for an additional charge. Contact UMI directly to order.

UMI®

Bell & Howell Information and Learning
300 North Zeeb Road, Ann Arbor, MI 48106-1346 USA
800-521-0600

UNIVERSITÉ DE SHERBROOKE
Faculté des sciences appliquées
Département de génie chimique

OPTIMISATION EXPÉRIMENTALE DE LA SPHÉROÏDISATION DES POUDRES MÉTALLIQUES ET CÉRAMIQUES PAR PLASMA INDUCTIF

EXPERIMENTAL OPTIMIZATION OF THE SPHEROIDIZATION OF METALLIC AND CERAMIC POWDERS WITH INDUCTION PLASMA

Mémoire de maîtrise ès sciences appliquées
Spécialité: génie chimique

Nicolas M. DIGNARD

Sherbrooke (Québec), CANADA

Septembre 1998

À ma famille

À la mémoire de mon grand-père, Léo

RÉSUMÉ

Une étude expérimentale de l'efficacité de sphéroïdisation des procédés par plasma inductif a été complétée. L'objectif principal étant d'obtenir des modèles qui pourraient être utilisés pour prédire l'efficacité de sphéroïdisation pour différents types de poudres sous différentes conditions d'opération des systèmes de plasma inductif. Les techniques de microscopie optique, microscopie électronique à balayage, sédigraphie et de diffraction rayon-X ont été utilisées pour l'analyse des poudres originales et des poudres traitées.

Des poudres de silice, d'alumine, d'oxyde de chrome, de zircone et de carbure de tungstène ont été utilisées pendant les expériences. Pour le traitement par plasma inductif, deux installations différentes on été utilisées. La première installation pouvait fournir une puissance maximale de 100 kW et opérait avec une fréquence de 0.3 MHz et la seconde pouvait fournir une puissance maximale de 50 kW et opérait avec une fréquence de 3 MHz. Les conditions d'opération on été choisies pour minimiser les réactions et l'évaporation des particules.

Les poudres traitées démontraient un phénomène de formation occasionnel de cavités internes dans les poudres traitées et un léger changement dans le diamètre moyen des particules traitées. Le modèle théorique prédit de façon satisfaisante l'efficacité de sphéroïdisation des poudres après que l'efficacité énergétique maximale a été atteinte. La dépendance des paramètres du model sur les propriétés thermodynamiques des poudres et sur les paramètres d'opération du plasma a été démontrée.

ABSTRACT

An experimental study of the spheroidization efficiency of powders in an induction plasma process was completed. The main objective being to develop a model which could be subsequently used for the prediction of the spheroidization efficiency for various powders under a wide range of plasma operating conditions. Throughout the study, optical microscopy, scanning electron microscopy, sedigraphy and X-ray diffraction were used to analyse the original and plasma treated powders.

Silica, alumina, chromium oxide, zirconia and tungsten carbide powders were the subject of systematic experimentation using two different plasma installations. One of the installation had a maximum available power of 100 kW with an operating frequency of 0.3 MHz while the other had a maximum available power of 50 kW with an operating frequency of 3 MHz. Operating conditions were varied such to minimize reactions and evaporation of powders.

The presence of internal cavities was observed in the treated particles along with a slight change in the mean particle diameter of the powders. The proposed model successfully predicts the spheroidization efficiency of the particles beyond a defined critical point known as the maximum energy efficiency point. The model parameters are shown to depend on the thermodynamic properties of the powders and on the induction plasma operating parameters.

ACKNOWLEDGEMENTS

I would like to express my appreciation to all who have contributed to the completion of this thesis. I would specially like to thank Prof. Maher I. Boulos for his support both information wise and financially. His latitude in enabling me to work in many areas even beyond the field of study, the experiences and extra learning opportunities offered are greatly appreciated.

All the members of the Plasma Technologies Research Centre (CRTP) were also of great resource. In particular, I would like to express my thanks to Serge Gagnon along with Marc Couture who both shared their experience and gave me all the support and information required to successfully design many reactors and complete my experimental work. Their patience is greatly appreciated.

The software wise support of Benoit Côté and Patricia Fournier are also appreciated for they were essential in moments were either megabytes or time were rare.

Finally, I want to thank all other students, both at the undergraduate and graduate level, which made life in the Sherbrooke area more than a simple enjoyment by offering a large variety of possibilities to unwind.

TABLE OF CONTENTS

LIST OF FIGURES

LIST OF TABLES

CHAPTER 1

INTRODUCTION

Since the earliest theoretical and experimental research in plasma technologies, some basic applications have been the subject of numerous investigations. The gradual widening of the fields of applications has been constant since. The earliest and simplest application was the heat treatment of particulates. This was the first step which could be easily used to evaluate the performance of this new high temperature technology. A technology which could be used with relatively small experimental or industrial set-ups. The following developments have included high performance materials with generally high melting temperatures. Some of the applications beyond the spheroidization of particles which have been developed are the spraying of high temperature resistant coatings and coatings with other specific properties which fulfilled the specific requirements of industries. These can be for protection from magnetic fields, electric fields, for the rebuilding of cutting tools or high performance machinery as for example, the rebuilding of specialized ball valves. In recent years, more specific applications have been developed. These include the coating of bioactive implants, the production of ultra fine powders and plasma chemical synthesis. One of the latest research areas developed with a very wide application field is the treatment of wastes.

All these technological advancements are done with a wide range of plasma generating techniques. The main plasma generation technique chosen for a specific procedure is dependant on the temperatures required. This is only one of the factors since there is a great number of variables which can influence the choice as the residence time required and the size or

accessibility of the apparatus for example. The main principles of plasma generation are thermal arc plasmas which can be with or without transferred arcs and thermal radio frequency discharges also known as high frequency induction plasmas [PFENDER et al., 1985]. Both have their particular advantages which usually determines which is used for the process in question.

For the spheroidization and densification of particles, h.f. induction plasmas is the preferred plasma generation method due to the longer residence time possible for the particles in the plasma and also it's ability to avoid the contamination of the product. The absence of contamination is because this plasma generation technique lacks the presence of electrodes unlike arc generation. The erosion of the electrodes introduces a foreign substance into the reactive system. This latest characteristic is of extreme importance in the production of high purity. Another characteristic of the induction plasma system is the easy introduction of the raw product in the core of the plasma. Most other methods must introduce the particulates from the outer regions of the plasmas. It must however be noted that recent advances in arc generation can now allow for the central injection of the particulate. It does however require a complicated and expensive torch design.

The spheroidization and densification of powders was one of the first uses of the plasma technology. It has therefore been very extensively studied theoretically. Mathematical modelling have been performed over the years in order to describe quantitatively the phenomenons involved in the process and to predict the outcome of the treatment. The optimization and prediction of the product output and quality is the essential information for industries. This is mainly due to the high cost of the technology and the desire to minimize pre-production lengthy experimentation

necessary for parameter optimization. The modelling of the induction plasma process has described quite well the phenomenons which occur during the processing of the materials. However, the prediction of the degree of melting and densification of the powder requires a good knowledge of the thermophysical properties of the material being treated which are not always available except for well studied materials. Most industrial applications are oriented towards the development of new advance materials with scarcely available physical properties. Other problems with modelling is that many approximations or simplifications which are usually made in the numerical calculations. Experimentally determined models can be used, on the other hand, to predict the resulting spheroidization and densification efficiencies and to predict the optimal operating conditions for a process. For the model to be practical, it should incorporate the principal thermophysical properties of the material treated. From this model, the spheroidization and densification efficiency and it's limits for a particular powder could be known based on the properties of the powders for a given set of plasma operating conditions.

Chapter 2 is dedicated to a literary review of h.f. induction plasma and the review of the necessary thermophysical properties which separates into distinct categories the powders. It also includes a review of the heat transfer methods to determine which are significant and what simplifications can be used in the model. The heat transfer methods are used to determine the energy balance but a discussion of the dynamics will also be completed. Chapter 2 ends with a review of previous works on powder spheroidization and densification. Chapter 3 will introduce mathematical models and their physical limits based on the properties of the particles for the process. It also introduces empirical equations which have been experimentally determined for the optimization and prediction of the spheroidization efficiency. Chapter 4 presents in details

the experimental set-ups used for the completion of the experiments. Chapter 5 will present the experimental results with an analysis of the treatment efficiency as a function of the powder feed rate. The results are compared with the predictions of the empirical models used. A summary and conclusion are presented in chapter 6.

CHAPTER 2

LITERATURE REVIEW

In the first part of this chapter, the generation of h.f. induction plasmas is presented. It is followed by a presentation of the thermophysical properties which influence the spheroidization process as well as the controlling heat transfer mechanisms.

2.1 H.F. Induction Plasmas

The earliest plasmas which were generated without electrodes appeared in the early sixties in the works of [REED, 1961]. He showed that a gas flowing in a cylindrical quartz tube could be maintained as a stable plasma at atmospheric conditions when submitted to an electromagnetic inductor. Since these early experiments, many others were performed to study h.f. induction plasma and also its applications to possible processes. Many of both the induction plasma and its applications have been completed since as presented by [BOULOS, 1991 and 1992, YOSHIDA et al., 1983 and FAUCHAIS, 1980].

For an induction torch as presented in Figure 2.1, the energy coupling between the electric generator and the plasma itself is done by a cylindrical induction coil. This eliminates the possibilities of product contamination by the plasma generation apparatus itself. This latest property of the induction torch also allows for the use of a wider variety of gases since the is no risks of these gases interacting with parts of the torch. It therefore opens widows of opportunities on many other chemically reactive systems.

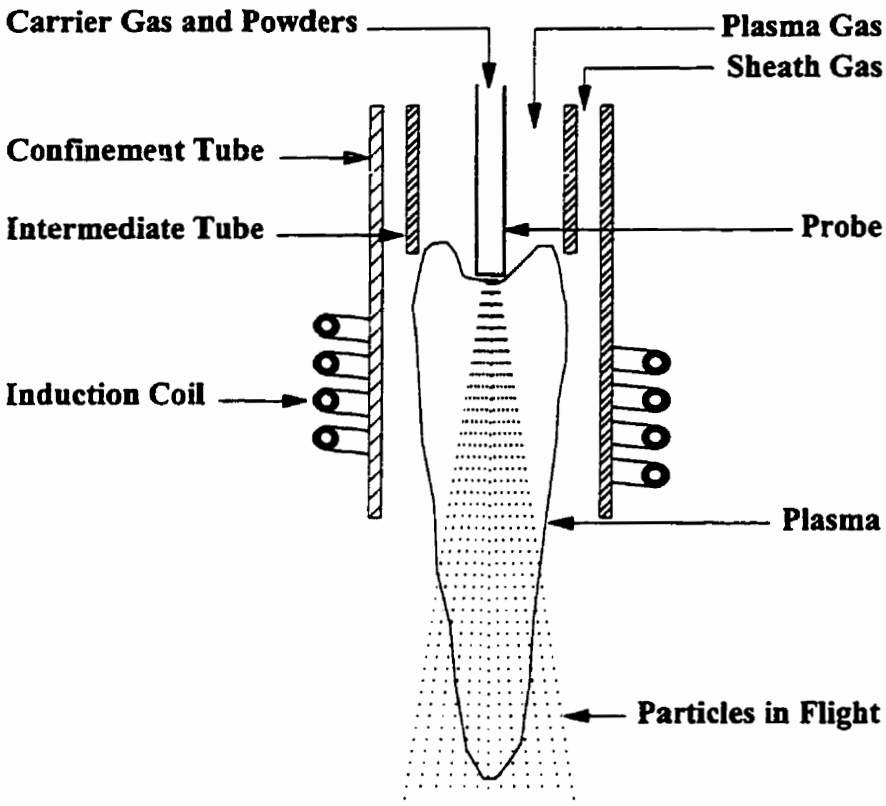

Figure 2.1 H.F. Induction plasma generation within the confinement tubes with an induction coil

2.1.1 H.F. Induction Plasma Characteristics

The induction plasmas have particular characteristics which are dependent of the operating conditions of the plasma torch and which can influence the process. The modification of each of the plasma torch parameter affects the efficiency of the torch and may also interactively modify other parameters if they are not maintained constant.

The power of an induction torch will determine the energy available to the process. However, in order to maintain a stable plasma, there is a minimum power required which is dependant on the other operating parameters of the induction torch as presented by [POOLE et

al., 1973]. The minimum sustaining power for a torch can range anywhere from a few watts to millions of kilowatts. Once the plasma is ignited and is stable, the increase of the power will result in the increase of the ionization of the plasma gas and subsequently will increase the energy available for the process. Regular h.f. electric generators can provide any power required up to its maximum capacity resulting in the possibility of a wide range of operating powers.

The frequency is actually the parameter which defines the h.f. induction plasmas. As mentioned earlier, it is also known as radio frequency plasmas and therefore sets the operating frequency in the range of 20 kHz up to 10 MHz. The frequency is also a variable which affects what is known as the skin dept. The skin dept is the thickness of the external cylindrical shell of the resulting load. It is the region of the plasma where the temperatures are the highest.

The frequency unlike the power can not be varied as easily. The induction plasma electric generators are build with a certain frequency which can be slightly modified. However, they are usually maintained a the predisposed frequency and other operating parameters are modified if different plasma conditions are required. This also results in different minimum operating power and pressures for different installations.

The pressure is an external parameter in that it must be controlled from the process chamber. Even though it is external, it has as much influence on the resulting plasma flame as does the power. The pressure has a physical effect on the plasma flame as it can increase it size or density. As for the power, there is also a maximum pressure allowable such to maintain a constant plasma. Reactor chambers may operate above or below atmospheric pressure depending

on the process requirements. The only complications are to maintain the desired pressures without contaminating either the inner or outer environments.

The other major parameter which influences the resulting plasma flame is the composition of the gases used in the torch. Argon is the gas with one of the lowest ionization energy which is readily available. It is generally the plasma gas used to start the induction torches as the minimum power and the maximum pressure required for the ignition of the plasma are optimal as presented in [POOLE et al., 1973]. Other gases as the sheath gas and the carrier gases are also introduced in the system for the process optimization and torch protection purposes.

The subsequent introduction of other gases or simply the substitution of the argon for other gases allows for a change in the thermophysical properties of the plasma gases. The main thermophysical properties of the gases which are of importance during the plasma induction process are the plasma density, enthalpy, specific heat, viscosity, thermal conductivity and the electric conductivity as presented in [BOULOS et al., 1994].

The other implications of the replacement of the plasma, carrier or sheath gases is that it allows for the introduction of gases not for their thermophysical properties but for reactive characteristics. With this possibility, many reactions have been studied and completed as presented by [PROULX et al., 1991a, GUO et al., 1995 and JIANG et al., 1995].

All four major parameters which affect the plasma flame properties and their minimum required operating conditions can be described graphically as shown in Figure 2.2.

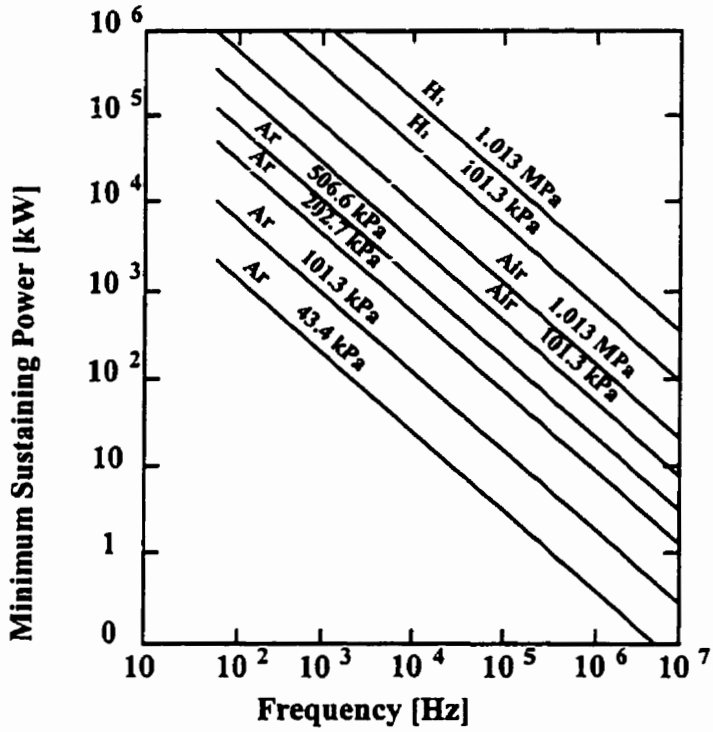

Figure 2.2 Minimum sustaining power for induction plasmas of different gases at different pressures as a function of the operating frequency

2.1.2 H.F. Induction Plasma Modelling

Since the early discovery of induction plasmas, modelling attempts have been done with ever increasingly powerful computers. In the early stages, the modelling was focused on the behaviour and properties of the plasma flame as presented in [BOULOS, 1976]. Combining the equations of motion, energy, electric and magnetic fields along with many assumptions many characteristics of the plasma induction process were determined. The flow fields which gave velocity profiles, the temperature, electric and magnetic fields were all obtained and therefore described fairly completely the plasma flame.

The introduction of particulate into the plasma flame complicated the modelling as it had and interactive behaviour with the plasma flame as presented by [BOULOS et al., 1974 and PROULX et al., 1985]. The introduction of particles into the plasma had for a purpose to melt them to spheroidized powders. However it was found that this particle loading had a very large cooling effect on the plasma flame and the amount of cooling had to be determined. New results had to be obtained as the particles distributions and paths within the plasma torch where now of significant importance.

The introduction of foreign matter in the plasma torch also brought new thermophysical changes to the plasma as it can be seen in [ESSOLTANI et al., 1993 and 1994]. The modelling had to include the change in thermophysical properties of plasma due to the presence of metallic vapours or any other impurities brought by the desired reaction. This will become ever more complex as the latest investigations for induction plasma technologies rely on the introduction of multiphase, multicomplexe compounds as in waste treatment or suspension plasma spraying.

2.1.3 H.F. Induction Plasma Torches and Installations

Induction plasma installations can generally be found in ranges of 10 to 100 kW. Some 400kW installations are however operational. The dimensions of the torch can vary from 3.5 to 10 cm diameter for the inner walls which are water cooled surrounded by a 3 to 7 turn induction coil. The radio frequency generally used for induction plasma generation varies between 200 kHz and 40 MHz. The plasma confining cylindrical tubes are now made of ceramics due to their improved thermal shock resistance which gives rise to longer life spans [BOULOS, 1991].

The gases are introduced in various modes and velocities. The plasma gas (central gas) is introduces tangentially and axially to stabilized the plasma discharge. The sheath gas is introduced axially with high velocities to reduce the thermal load on the inner surface of the plasma confinement ceramic tube. The carrier gas is injected axially in the centre of the torch with an injection probe which is cooled with high pressured water. It is injected centrally since it is the region with the highest temperature. The total volumetric flow rate of gases can vary between 100 and 150 slpm depending on the plasma power rating.

The maximum temperatures attained in r.f. induction plasma torches can vary between 8000 to 12000 K and the residence time of the gases can range from 10 to 20 ms.

All these required installations and operating materials (gases, electricity, water cooling, pressure maintain) do represent many expenses. This is why the r.f. induction plasma technology is generally known as an expensive technology. However, this is why it is used mainly in areas of high performance materials or where it is absolutely necessary. In the first case, there is a high added value to the product which renders the process economically viable. In cases where the technology is necessary, the product must be treated and it is one of the few technologies available to complete the task. It is why the used of the induction plasma technology must be well evaluated before using it as presented by [JACQ et al., 1992].

2.2 **Thermophysical Properties**

To understand the heat transfer which occurs in the plasma, the thermophysical properties of the system are required. These can be divide clearly in two different categories when it comes

to the heat treatment of particulate. The first category is the thermophysical properties of the plasma itself while the other category is the thermophysical properties of the powders.

2.2.1 Thermophysical Properties of the Plasma

The thermophysical properties of the plasma are dependant on the major parameters mentioned in section 2.1.1. Since they are also a function of temperature, most properties vary within the plasma itself. This complicates the macroscopic evaluation of such a process. In a real space analysis, the density, enthalpy, specific heat, viscosity, thermal conductivity and electric conductivity are different at every point in the plasma torch (neglecting the cylindrical symmetry). The amount of data required in such an analysis is astronomical as it is presented in [BOULOS et al., 1994].

Another aspect which complicates the evaluation of the properties of the plasma is that depending on the plasma operating condition, the temperature profile changes as seen in [MOSTAGHIMI et al., 1985 and 1990 and BOULOS, 1976]. This means that for every different torch or power supply of a different frequency, all of the plasma thermophysical properties will change.

2.2.2 Thermophysical Properties of the Powders

Unlike the properties for the plasma flame, a set of thermophysical properties are unique for every different powders. Some of the properties are characteristic of powders to the point of separating them in different categories. That is the case for ceramics powders and metallic powders which can be primarily differentiated by their thermal conductivity. The metallic

powder usually having much higher thermal conductivity as mentioned in [DIGNARD et al., 1997a].

The basic properties which are of interest for the process and that are known and readily available are the thermal conductivity, the density, the specific heat, the melting temperature, the vaporization temperature, the latent heat of fusion, the latent heat of vaporization and the particulate size or diameters as presented in [DIGNARD et al., 1997b]. There are many more other properties known but that are of less or negligible importance. All these parameters and thermophysical properties of the plasma are needed for the evaluation of the plasma particle heat transfer phenomenon.

2.3 **Heat Transfer mechanisms**

In the plasma processing of materials, there are three major heat transfer mechanisms which account for the energy transfer between the plasma, its surroundings and the particulate which are to be treated. The three major mechanisms are the heat transfer by conduction, by convection and by radiation [ESSOLTANI et al., 1993].

2.3.1 Conduction

In the plasma processing of powders, heat conduction phenomenon are observed either between the plasma and the inner walls of the plasma confinement tube, between the plasma and the particles, within the plasma itself due to the high temperature gradients and in the particles themselves. Since the process considered involves the melting and resolidification of the particles, the transfer of the energy from the plasma to the particle and the heat distribution within

the particles are the controlling phenomenon that affect directly the spheroidization efficiency. The transfer from the plasma to the particle is governed by the classic heat transfer equation modified for this application which is presented in Equation 2-1 obtained from [BOURDIN et al., 1983]:

$$q = \frac{2\bar{k}}{d_0}(T_\infty - T_S) \qquad (2\text{-}1)$$

Where q is the heat flux to the surface of the particle, $\bar{k}$ is the integrated mean thermal conductivity of the plasma gas, d_0 is the particle diameter, T_∞ is the free stream plasma temperature and T_S is particle surface temperature.

To obtain the temperature in the particle, the transient heat transfer equation must be applied to particle itself. This will allow to determine a temperature profile within the particle and therefore determine if the whole particle was molten by the process. Unless the particle has an infinite conductivity, there shall always be a temperature gradient between the particle's surface temperature and the particle's central temperature. The equation has to be solved with boundary conditions and gives a temperature profile as a function of the radius. However, if the Biot number is lower than 0.02, the temperature gradient can be neglected as proven in [BOURDIN et al., 1983].

2.3.2 Convection

An equation for the convection heat transfer is quite easily obtainable. It is actually included in the equation for heat transfer by conduction. Since it also depends on the temperature difference between the surface and the free stream temperature, the contribution of the heat transfer by convection is included in the overall heat transfer coefficient h. It must be noted that in h.f. induction plasmas, the velocities of the gases are generally quite low ranging from 10 to 40 m\s as shown in [BOULOS, 1976]. It can therefore be seen that the heat transfer by convection is much less than the heat transfer by conduction.

2.3.3 Radiation

Radiation within a plasma can get quite complicated. In some cases, up to 45% of the initial plasma energy is lost to the surroundings by radiation as presented in [PROULX, 1991b]. When heat transfer from the particles to the surrounding is involved, the radiative heat transfer equation is presented as Equation 2-2 from [BOULOS, 1978]:

$$q = \in\sigma(T_s^4 - T_a^4) \qquad (2\text{-}2)$$

Where $\in$ is the particle emmissivity and σ is the Stefan-Boltzmann constant and T_a is the ambiant walls temperature.

However, even though the effect of radiation on the plasma energy balance itself is important, it turns out that the importance of the radiation to the heat transfer to the particles can

be neglected unless the particles' surface temperatures exceed 2000. This is particularly important when dealing with the melting of high melting point refractory materials. Radiation heat transfer is also greatly influenced by the presence of metallic vapour in the plasma as showed by [ESSOLTANI et al., 1990,1993 and 1994 and VARDELLE et al., 1990] which increases considerably radiative energy losses from the plasma.

2.4 Energy Balance

When the particulate matter is introduced into the plasma, the resulting powders will be completely spheroidized if a certain thermodynamic stage was reached during the process. This critical point is the minimum requirement for the spheroidization process to be completed. It does however, for optimization purposes, also represent a point beyond which overheating of the particles results in a waste of energy and of material due to the subsequent evaporation of the particle as is presented in [MCKELLIGET, 1992 and BOURDIN, 1983].

The equilibrium point that is required is obviously material dependant. It is not a true equilibrium but simply a stage where there is no more fusion of the particle. The only changing parameters from this point on is the temperature of the particle, up to its evaporation point, followed by changes in the size of the particle due to the evaporation of its outer surface. This latest phenomenon is one which is not desired during such processes. The determination of the energy required to reach this equilibrium point is done with an energy balance on the initial particles. Equation 2-3 represents the total energy required to first heat the particle to the melting temperature and to then completly melt the particle. The particle is then free to assume its spherical shape due to the minimization of the surface energy as presented in [MUNZ, 1996].

$$q = mC_p(T_m - T_0) + m\lambda_m \qquad (2\text{-}3)$$

Where q is the energy transfer required to the particle to reach the critical point, m is the mass of the particle, C_p is the specific heat of the material, T_m is the melting temperature of the material, T_0 is the initial temperature of the particle and λ_m is the latent heat of fusion of the material.

The energy transferred to the particle does not however distribute itself as mentioned by the equation. As shown by [BOURDIN, 1983], since the conductivity of materials are never infinite, there is an actual gradient of temperature within the particle. There is the heating of the liquid phase to a temperature higher than that of the melting temperature and in cases of large temperature gradients, there can be an evaporation of a fraction of the material.

Deviation from Equation 2-3 can occur depending on the thermophysical properties of the material considered. It must therefore simply be used as a reference point for comparison. Other factors as for example the kinetics of both the energy transfer and the mass transfer within the particle itself can also be limiting.

2.5 Dynamics of the Powder Spheroidization

As mentioned earlier, even though the thermodynamic state wanted is known, there is still the questions of dynamics. In the induction plasma processing of powders, their is two distinct

dynamics phenomenon present as shown in [PROULX et al., 1985 and 1987, MUNZ, 1996 and BOULOS, 1978]. There is the dynamics which control the energy transfer and the dynamics which control the mass transfer.

2.5.1 Heat Transfer Controlled Phenomenon

The key parameter of the heat transfer dynamics is the residence time of the particles in the plasma discharge. It is known that for h.f. induction plasmas, the average residence time for a particle can vary from 5 to 20 milliseconds as presented by [COULOMBE, 1994]. However, in the same plasma, the particles will not all travel by the same pathways. This has for effect to create many different residence times for various particles with an exposure to different temperatures as seen in [PFENDER, 1989, PROULX et al., 1987 and BOULOS, 1978]. The different trajectories are also greatly affected by the size of the particle

Other parameters which influence the residence time are recirculations present in the plasma due to the magnetic field and the inter particle collisions which are frequent under dense loading conditions as previously shown in [MOSTAGHIMI et al., 1985].

Knowing the average residence time for r.f. induction plasmas, it is possible to estimate the quantity of energy which may be transferred to the particles. This can be done using the thermophysical properties of the particles and plasma combined with a chosen average residence time for the particular torch. The result can be used to determine if either the heat transfer dynamics or the thermodynamic critical point will be the limiting factor for the processing of the selected powder.

2.5.2 Mass Transfer Controlled Phenomenon

The dynamics of mass transfer determine the time required for the complete melting of the particle. The thermophysical properties which are involved in such calculation are the molten liquid's density, surface tension and viscosity as presented by [CLIFT, 1978]. The main dimensionless numbers used to determine the final shape of the particles are the Reynolds number, the Morton number and the Eotvos number. Even though the optimal final shape relative to the minimization of energy is spherical, forces from the drag, impurities or internal motion for example may affect the final shape of the particles.

However, as mentioned, most thermophysical properties are not available for such calculations. Previous experiments have very rarely shown final shapes other than spheres. If other shapes as ellipses are in the resulting powders, the usual observation is that the particle did not have the time to completely melt during the heating process. This is why most estimation of spheroidization efficiency of systems on particles are usually done experimentally as done by [DIGNARD, 1997a, 1997b and 1998, FAN, 1994 and JIANG, 1994].

2.6 Spheroidization of Powders

Previous works have been done on the spheroidization of particles both experimentally and theoretically. Theoretical works, mostly numerical calculations, have been focused on the energy transfer to the particles during the induction plasma or arc plasma processes. There is very little modelling which can predict if the particles will be spheroidized or more precisely, determining the actual spheroidization efficiency of the plasma as seen in [MCKELLIGET, 1992, BOULOS, 1978, PROULX et al., 1985 and 1987, and PFENDER, 1989]. This lack of practical

results requires attempts at an experimentally determined technique which could be used to predict and therefore optimize the spheroidization of particles..

Many experimental studies have also already been completed in the area of spheroidization of particles as done by [ISHIGAKI et al., 1991, FAN, 1994 and JIANG, 1994]. However, most experimental approaches are directed at only one material since their experimental studies were aimed at subsequent use of the information. Their objectives were mostly oriented at the future deposition of the powders into substrates. The approach is that knowing that the particles have been spheroidized, the critical point (thermodynamically) has been attained and consequently a complete melting of the particles is assumed when 100% spheroidization efficiency is obtained.

In the last decade, the production of high added value powders with constant size, properties and quality has been increasing. This trend follows the development in high performance materials and therefore creates also a demand for high quality pure raw products. From this avenue, the necessity for the obtention of tools for the prediction and optimization of the spheroidization efficiency for many materials gains ever more importance.

2.7 **Densification of Powders**

The densification of the powders while processing them by induction plasma has for long been an added advantage to the plasma technology. It is well known experimentally for the densification of agglomerates. The undensified original powders can be initially agglomerated by

techniques like spray-drying and consequently submitted to a plasma treatment to densify the powders as presented in [PAWLOWSKI, 1995].

The densification of agglomerates by induction plasmas has also opened new fields in the areas of suspensions plasma processing. This process is the precursor to suspension plasma spraying. The process enables to create either powders from a mixture of reactive components which are stabilized in a suspension as shown in [BOUYER, 1997a and 1997b]. In the first steps of the process, the mixture is atomized for the rapid evaporation of the liquid and to allow the formation of small spherical shells which can subsequently be densified.

There is however a physical limit to the possible densification of the powders other than the theoretical density of the original materials. This has been theoretically studied and also supported by experimental work as presented by [KLIMA et al., 1997]. A mathematical model was developed to determine the radius of the cavity which could remain at the interior of the spherical particle after the heat treatment. The initial parameters on which this theory is based is the difference in densities between the material in its solid phase and in its liquid phase. The formation of this cavity is initiated during the cooling of the particles. As the exterior of the molten sphere solidifies, the pressure in the remaining melted material will decrease and eventually possibly create a cavity. The possible cavity would be due to the bubbling of the remaining molten material. Equation 2-4 can be used for an estimation of the radius of the resulting cavity within the obtained sphere.

$$\frac{R_c}{R_0} = \left(1 - \frac{\rho_m}{\rho_s}\right)^{\frac{1}{3}} \qquad (2\text{-}4)$$

Where R_c is the radius of the final cavity, R_0 is the radius of the initial droplet (molten material), ρm is the density of the melted phase and ρs is the density of the solid phase. These results mean that a spherical powder could in some cases, be less dense than the theoretical density of the material. It must be noted that the possibility of reabsorption of a gas was not considered. This latest assumption is applicable to the case of induction plasma processes since the solidification of the particles is rapid. This joined to the relatively low diffusion coefficients of liquid materials of metals as presented by [SCHEIBEL, 1954 and WILKE, 1949] could explain the presence of cavities within some processed spherical powders.

CHAPTER 3

DEVELOPMENT OF SPHEROIDIZATION MODELS

The development of models which can predict the spheroidization efficiency of the injected powders as a function of the powder feed rate is required. A model based on the energy transfer equation and other phenomena occurring during the process would be preferred to an empirical model. However, even if such a model will be developed, the previous lack of similar models even by numerical analysis can presume that the empirical models will be useful.

3.1 Energy Transfer Model

An initial description of occurring phenomenons is required before modelling them. The changes with which the model is concerned occur within the particles. The initial energy transferred to the particle will be used for the heating of the material up to its melting temperature. Thereafter, the melting of the solid phase into the liquid phase will occur. Even though the heating of the liquid phase and the subsequent evaporation of some material are not desired, they do occur since no material has an infinite thermal conductivity. These fours steps are described in Figure 3.1 by presenting the temperature profile of the particle as a function of its specific enthalpy for a case of infinite thermal conductivity.

3.1.1 The Minimum Energy Requirements

With the first two stages of this process, and estimation of the required energy to be transferred to the particles can be obtained. Since this resulting value is particular for every

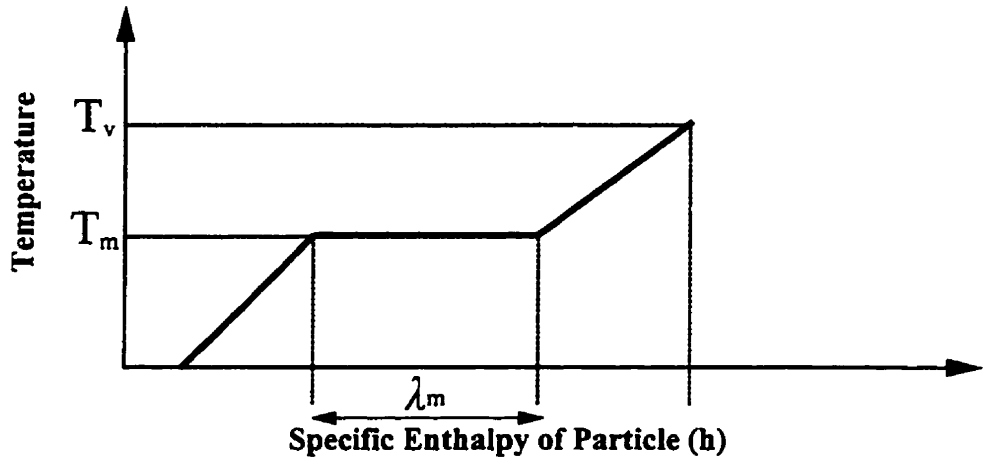

Figure 3.1 Temperature history of the particle during heating versus its specific enthalpy

different material used, it is a limiting parameter for the process. The minimum energy transfer to the particles can therefore be described by Equation 3-1.

$$Q = \dot{m} \cdot C_p(T_m - T_0) + \dot{m} \cdot \lambda_m \qquad (3\text{-}1)$$

Where Q is the minimum energy transfer required, $\dot{m}$ is the powder feed rate, C_p is the specific heat of the material, T_m is its melting temperature, T_0 is the initial temperature of the powder and λ_m is the latent heat of fusion of the material.

The total energy transfer required for the complete melting of a powder will therefore increase linearly as a function of the powder feed rate. However, since the energy available from the plasma diminishes with an increasing load because of the cooling effect, a net reduction of the melting and therefore spheroidization efficiency will occur after a critical value of the powder

feed rate. This value will be attained when the energy which can be absorbed from the plasma is equal to the minimum energy transfer required by the particles. Beyond this critical point, the spheroidization efficiency will decrease with the increase of the powder feed rate.

3.1.2 Energy Transferred From the Plasma to the Particle

Now that a critical parameter has been determined for the particles, the energy which can be transferred to the particles must be determined. To do so, an evaluation of the efficiency of the r.f. induction plasma installation must be done. Two methods can generally be used. Firstly, if an average temperature for the plasma discharge can be determined, a general energy balance can be used. Using the assumption that during the travel of the particle through the plasma, the integral mean value of the thermal conductivity across the boundary layer is the only spatially varying plasma parameter, the heat net flux to the particle, q, can be describe by Equation 3-2.

$$q = \frac{2k}{d_0}(T_\infty - T_p) - \epsilon\sigma(T_p^4 - T_a^4) \qquad (3\text{-}2)$$

Where k is the integrated mean thermal conductivity of the boundary layer, d_0 is the powders mean diameter, T_∞ is the plasma average temperature, ϵ is the emissivity, σ is the Stefan-Boltzman constant, T_p is the particle temperature and T_a is the ambiant wall temperature.

However, since the average temperature changes with increasing powder feed rate due to the cooling effect of the loading, this method can only be used for comparison between similar

plasma loading conditions. It can not be used to predict the process efficiency as a function of the powder feed rate without an estimation of the resulting average temperature changes caused by the overloading. Equation 3-2 can however be used to determine a parameter describing the energy transfer to a single particle for a desired average temperature.

3.1.3 The Melting and Spheroidization Efficiencies

The energy transferred to a single particle can be used to determine if a specific powder with its thermophysical properties can actually be melted by the induction plasma. Since most of the heat losses from the particles are by radiation, it is normal to expect that larger particles can not attain an equilibrium temperature equivalent to smaller particles. This can be observed when simulating the heating of particles in a plasma with an infinite residence time. The results represent the maximum equilibrium temperature than can be attained by a particle of known size independently of the particles thermophysical properties except for its emissivity. The effect of the size of particles on this possible equilibrium temperature is show in Figure 3.2 for particles with an emissivity of 1 in a pure argon plasma.

From the results in Figure 3.2, we can see that an average residence time has to be known or estimated since not all particles can be melted as shown. It is known however, that residence times ranging from 5 to 20 ms are common for r.f. induction plasmas. So for an estimate of the maximum energy transferred to the particle, a value of 10 ms is taken. Comparing this heat flux to the minimum energy required represented in Equation 3-1, we obtain Equation 3-3. Equation 3-3 represents an estimate of the ratio between the energy transferred to the particle and the minimum energy required for the melting and spheroidization of the particles.

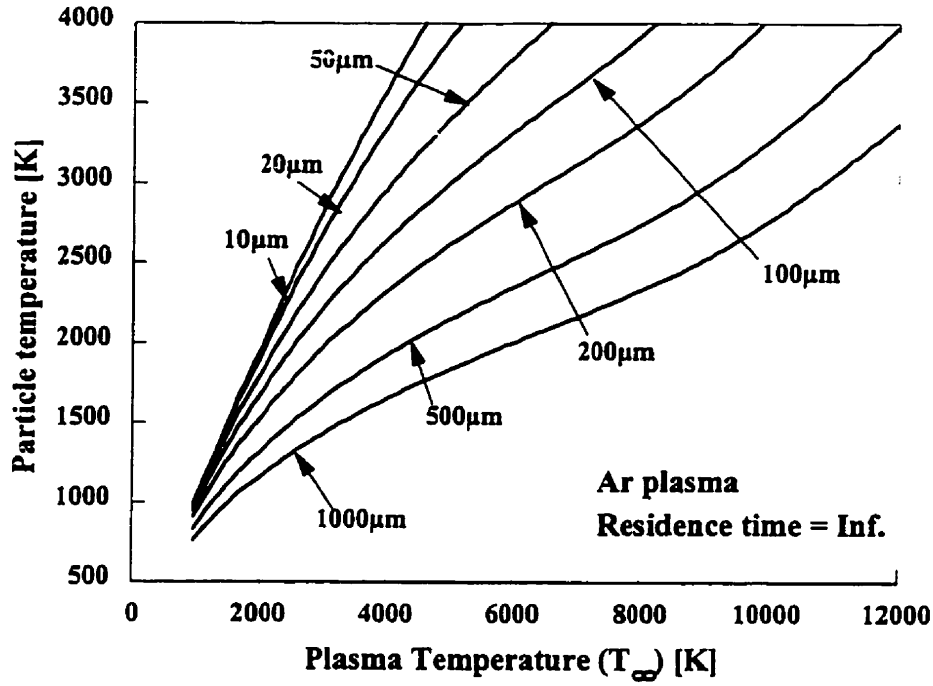

Figure 3.2 The maximum temperature attained by particles of various size with infinite residence time in an argon plasma of various average temperature

$$Ratio = \frac{\frac{6\dot{m}\Delta t^2}{\rho d_0^2 t_f}\int_0^{t_f} 2k(T_\infty - T_p) - \epsilon\sigma(T_p^4 - T_a^4)dt}{\dot{m}\Delta t[C_p(T_m - T_0) + \lambda_m]} \qquad (3\text{-}3)$$

Where Δt is the residence time chosen (10 ms), ρ is the density of the powder and t_f is the time required to melt the particle or the residence time if the time required to melt the particle is greater than the residence time.

If the ration is much lower than 1, the melting of all the powders will not be possible. However, if the ratio is equal to 1, the melting of the powders at low feed rates is possible since the ratio is not a function of the feed rate. It must be noted that as it is defined, the ration can not be greater than 1. However, it can be seen that if the residence time is long enough for the

melting of the particles, the ratio is as mentioned equal to 1. As the diameter for the particle is increased, a maximum diameter at which the particle can be melted will be attained and the efficiency of the system will subsequently diminish which is represented by the reduction of the ratio. This is due to the ratio being a function of the powders mean diameter. We can also notice that the ratio is dependant on the plasma average free stream temperature. It is therefore not accurate for cases where there is cooling effects due to the loading of the plasma. The importance of this effect can however be seen with Equation 3-3. By verifying the ratio with various free-stream plasma temperatures, the effect of a reduction in the average free-stream temperature by loading can therefore be observed. The only missing information is the actual amount of cooling due to the variation in feed rate.

To evaluate the effect of the chosen residence time on the resulting efficiencies, an evaluation of the latest can be performed for the powders which will be used. Since the residence time required depends not only on the size of the particles but also on the thermophysical properties of the materials, both must be taken into account. From Figure 3.3 which represent the required residence time for various kinds of powders as a function of the mean diameter, it can be seen that there are limiting diameters for the powders. This limiting diameter represent the diameter where a small increase in this one results in a large required increase in the needed residence time. Since that in the experimental cases, the residence times are similar from one powder to the next, we therefore know which materials are most likely to have acquired a sufficient amount of energy for their complete melting.

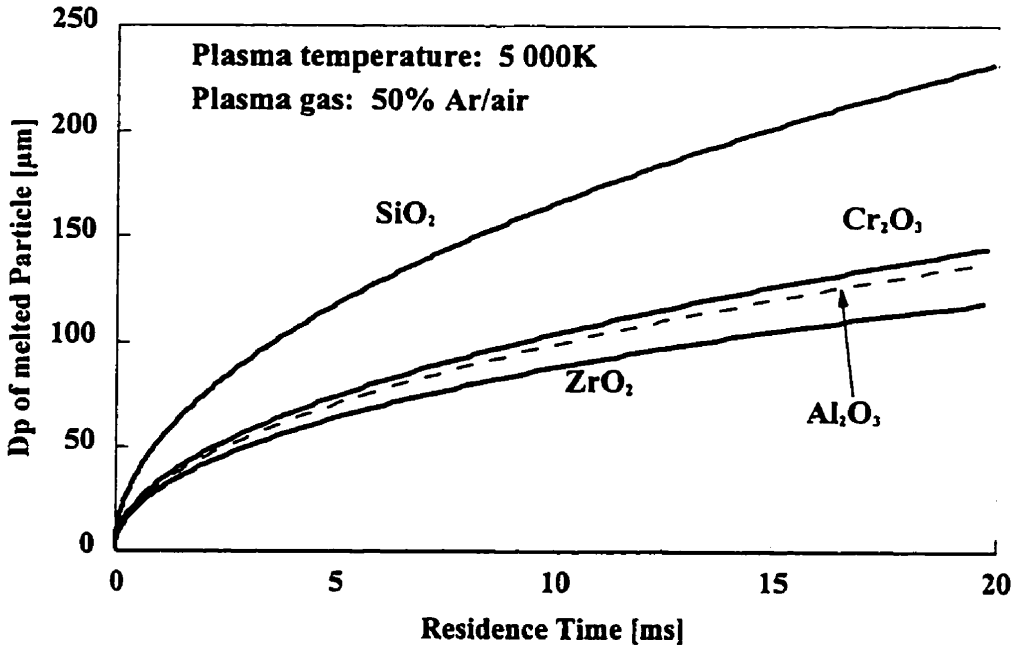

Figure 3.3 Dependency of the diameter of various powders as a function of the residence time

The second method which can be used to evaluate the melting and spheroidization efficiency is a macroscopic approach. It has been experimentally tested that 70% of the power generated by the r.f. induction plasma installation is actually transferred into plasma energy. From [PROULX, 1987], it has been determined that 13 to 18% of the total plasma power could be absorbed by the particles for certain cases. The main point to retain is that initially, at low feed rates, the percentage is actually lower. However, the equilibrium is quickly reach at a certain key feed rate and does not change significantly thereafter. These results do include the cooling of the plasma flame. Therefore, from the combination of both these estimates, we can obtain the maximum energy which can be absorbed by the particles for the particular system. Knowing the required energy to completely melt the particles, and estimate of the spheroidization percentage can be obtain. The only unknown parameter is the actual energy which can be

absorbed by the particles for a particular system. So once it is known that the particles have the required thermophysical properties and time to reach the spheroidization stage under no loading as shown by Equation 3-3, Equation 3-4 would allow the estimation of the spheroidization efficiency of the induction plasma process for the powders. It is the ratio of the transferred energy to the minimum energy required for the melting process. As the initial equations were estimate, a correcting factor which has to be determine will have to be used to optimize the model.

$$Efficiency = \frac{0.11Z(Pw)}{\left[\dot{m}C_p(T_m - T_0) + \dot{m}\lambda\right]} \tag{3-4}$$

Where Pw is the power supplied by the generator and Z is the correction factor. It must be noted that if the result is above 1, it simply reflects that the spheroidization efficiency should be 100%. The factor of 0.11 present is simply the average of previous works such to minimize the importance of the correction factor.

3.2 Empirical Model

The choice of the empirical model to be applied is initially based on the behaviour expected for the experimental results. In the case of the spheroidization efficiency, we can expect for particles with thermophysical properties that allows them to be completely melted to have an efficiency of 100% until a critical feed rate is reached. After this critical feed rate, we can expect a gradual decrease in the efficiency of the system. It is also expected that an actual 0% efficiency will only occur at extreme feed rates due to the small but finite chance that a few particles with

preferential contact with the plasma flame will remain present. So the empirical model which will be used to attempt a prediction of the spheroidization efficiency is presented in Equation 3-5.

$$\Theta = \frac{\Theta_0}{[1+(\omega F)^2]^n} \tag{3-5}$$

Where F is the powder feed rate in g/min, Θ_0, ω, and n are the characteristic parameters of the equations. We can observe that for a case where there is an infinitely small feed rate (few or single particle) the spheroidization efficiency is simply equal to Θ_0 which is 100% for particles with thermophysical properties that allows the particles to be completely melted during its flight through the plasma. The other two parameters do not have explicit physical representation as does Θ_0 which represent the efficiency of the system to melt a single particle.

The model suggested does however apply itself only for one set of experimental data. This meaning that once a set of efficiencies has been obtain, the parameters of the model can in turn be determined by an optimization of the fitting. The obtain parameters can be applied in the future only for powders of identical thermophysical properties, diameter included. This is useful for a process where the raw powders properties are constant but it lacks any flexibility for variations in either diameter or thermophysical properties.

3.3 Experimental Evaluation of the Model Parameters

The use of semi-empirical model is to isolated one or many variable of the process in order to identify their effect on the observed parameter. For the spheroidization of particles, the

key parameters for the thermophysical properties of the powders are the density, the thermal conductivity, the specific heat, the melting temperature, the latent heat of fusion and the mean diameter of the particles. It must be noted that many other parameters could be identified but limiting the number of variables has for purpose to simplify the resulting model.

3.3.1 Mean Diameter Based Empirical Model

The only parameter which can be isolated for the particles is the particles mean diameter as all the other thermophysical properties vary between the different material and can not be isolated. Therefore another model can presented as shown in Equation 3-6.

$$\Theta = \frac{\Theta_d D_p^{\Psi_1}}{\left[1+(\omega_d D_p^{\Psi_2} F)^2\right]^{n_d} D_p^{\Psi_3}} \tag{3-6}$$

Where the subscript $_d$ relates to the model with the isolation of the mean diameter and Ψ_x is the function which describes the effect of only the diameter on the efficiency of the system.

To obtain a relation for Ψ_x, experiments of with identical plasma conditions must be performed. These experiments ought to vary only in the mean diameter of the particles. The particles will have to be of a certain material with known constant thermophysical properties. Once the effect of the diameter on the spheroidization efficiency is known, the function is introduced in the model and the new values of the parameters can be determine. It must be noted that this model will be useful when a process is used with constant plasma conditions and with powders of identical thermophysical properties. If the raw powders do change in mean diameter

during a period of production, the process can be re-optimized with the help of the model. The remaining parameters which can not be predicted is the other thermophysical properties mentioned earlier.

3.3.2 Thermophysical Properties Based Empirical Model

This model is the logical approach following the model presented in Equation 3-6. The objective of this following model is to isolate the contribution of all the other thermophysical parameters on each of the three model parameters. The remaining unknown parameters will therefore only be function of the operating plasma conditions as is shown in Equation 3-7.

$$\Theta = \frac{\Theta_T D_p^{\Psi 1} \rho^a k^b C_p^c T_m^d \lambda_m^e T_v^f}{\left[1+(\omega_T \rho^g k^h C_p^i T_m^j \lambda_m^q T_v^r D_p^{\Psi 2} F)^2\right]^{n_T} D_p^{\Psi 3} \rho^s k^t C_p^u T_m^v \lambda_m^w T_v^x} \tag{3-7}$$

Where the exponents of the thermophysical properties are constants and the subscript $_T$ relates to the model containing all the thermophysical properties.

The obtain model might look very complicated but since most parameters are constant, the use of the model will be quite simple and relies only on the thermophysical properties of the powders. It must be noted that to obtain the values of the constants presented in the model, experiments with various powders (i.e. different thermophysical properties) must be completed under identical plasma conditions. This latest condition is due to the necessity to identify the remaining unknown parameters Θ_T, ω_T and n_T. Once the experiments are complete, the fitting of the model on the data must be optimized while the constants a-j and q-x are identical for all the

powders used and therefore determining the effect of each individual thermophysical property on each original parameter of the model. The resulting model should therefore be useful to predict the process efficiency for any powders under the specified plasma conditions. The only parameters to be determined subsequently would be the three base parameters. Once these would be determine for a plasma operating condition, the prediction of the spheroidization efficiency could be obtained. The model can also be used to isolate the variable which have the greatest effect on the process by comparing the exponents of these.

CHAPTER 4

EXPERIMENTAL APPARATUS AND OPERATING CONDITIONS

In the first parts of this chapter, the spheroidization experimental set-ups shall be described. It will be followed by a description of the powder feeders used during the processing of the various powders. The equipment used for the analysis of raw and resulting powders will also be presented.

4.1 Plasma Spheroidization Installations

Figure 4.1 and Figure 4.2 are schematic representations of the two complete r.f. induction plasma installations used in the present study. Figure 4.1 represents the 3 MHz frequency set-up with a maximum available power of 50 kW. Figure 4.2 represents the 0.3 MHz frequency set-up with a maximum output power of 100 kW. Both installations also include an induction plasma torch, a vacuum system, a reaction chamber, powder collecting systems and controls for the gas flow-rates.

4.1.1 Induction Plasma Torch

A schematic diagram of the plasma induction torch is presented in Figure 4.3. The inner walls of the torch are made of a cylindrical ceramic tube with an inner diameter of 50 mm. The ceramic wall is surrounded by the induction coil which had either four or five turns depending on the composition of the gases injected in the torch. The gases are introduced in the central region of the torch through a distributor which is located at the top of the torch. The sheath gas (Q3) is

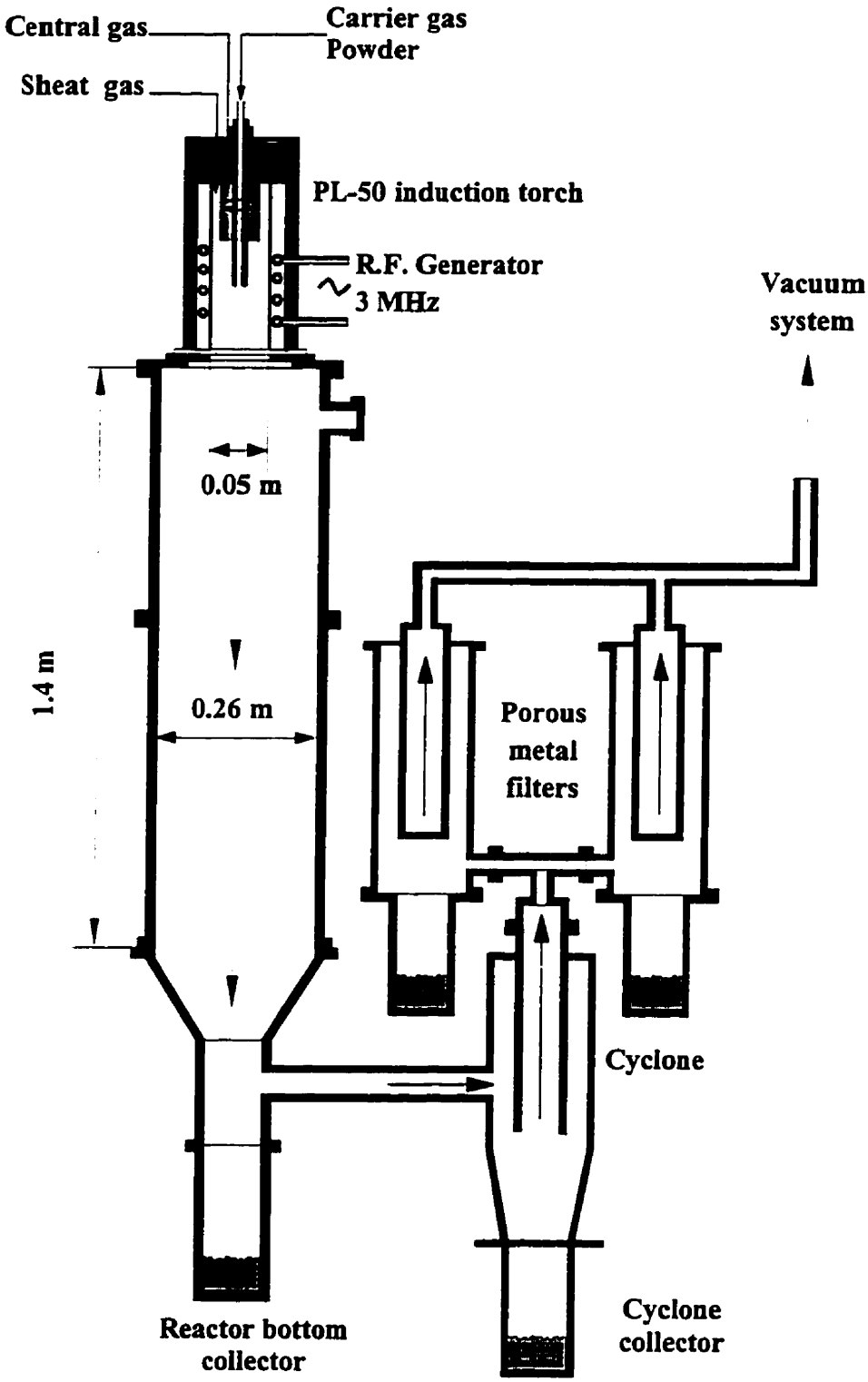

Figure 4.1 Schematic representation of the 3 MHz experimental set-up

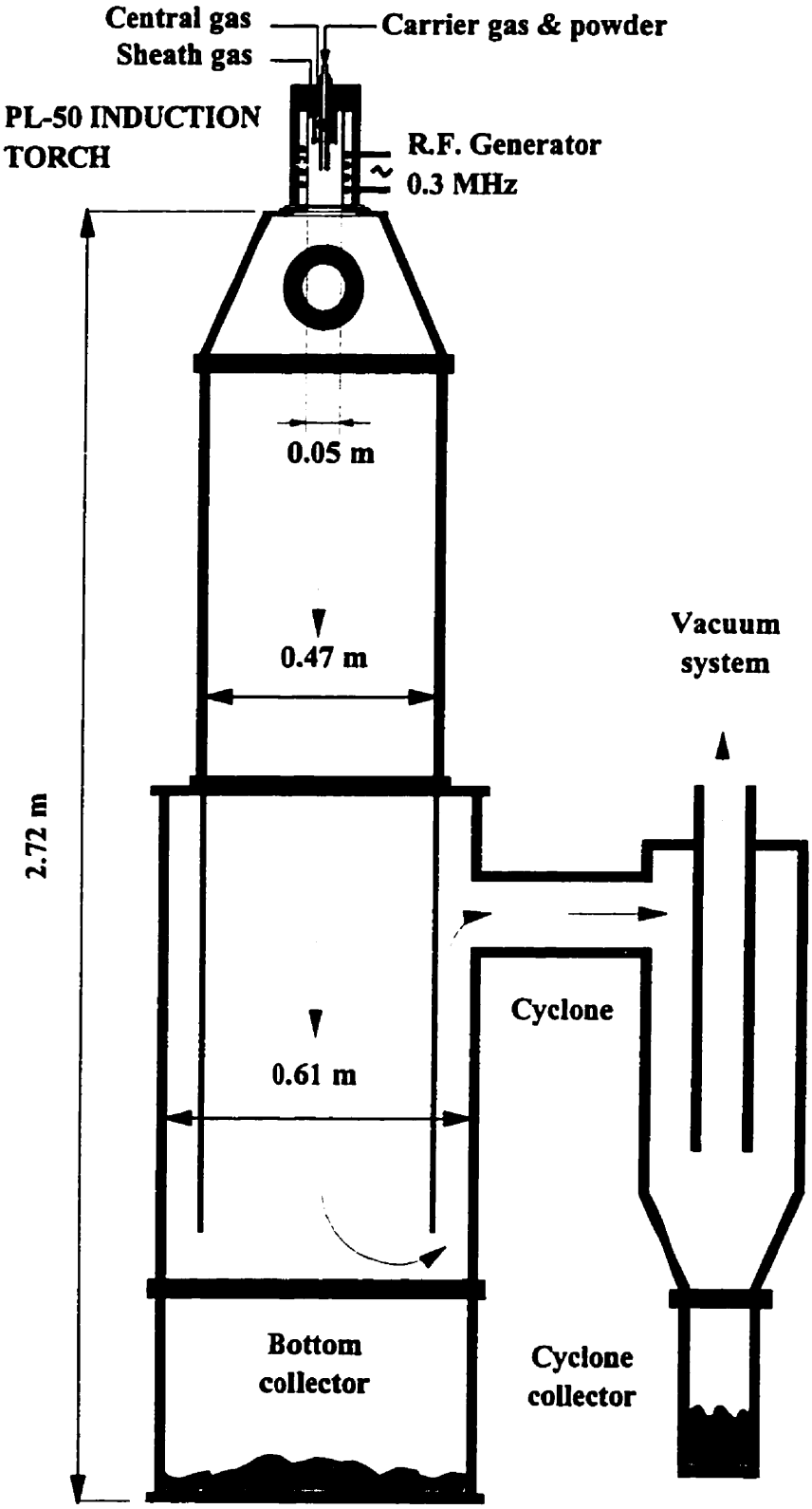

Figure 4.2 Schematic representation of the 0.3 MHz experimental set-up

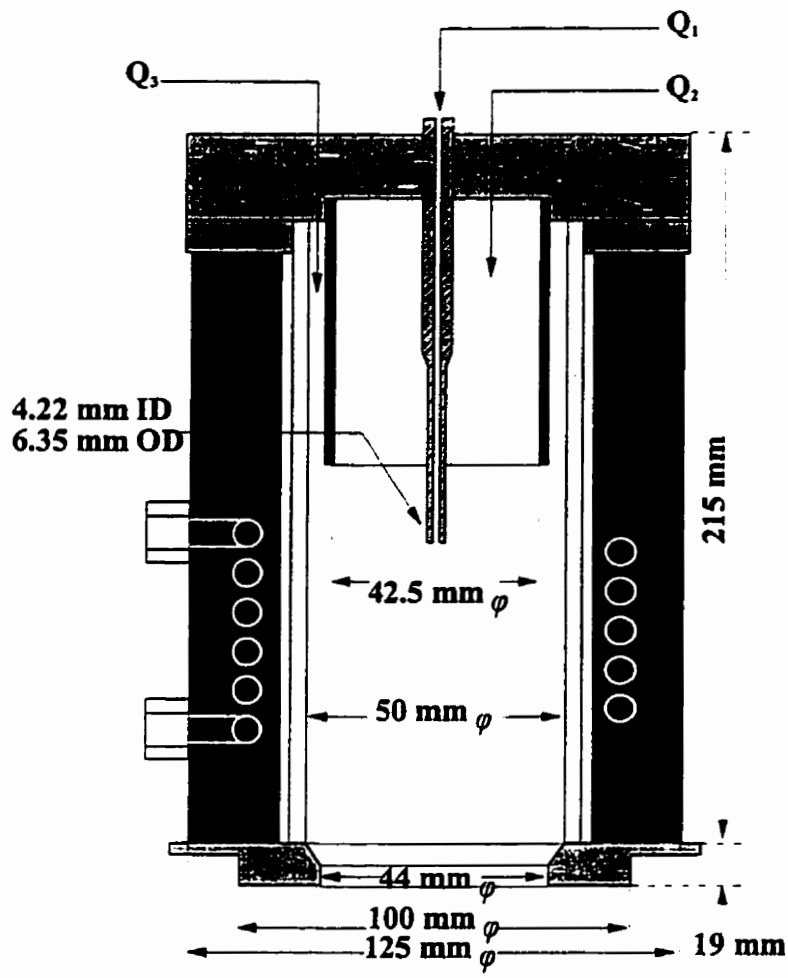

Figure 4.3 Schematic diagram of the induction plasma torch

injected along the ceramic tube to reduce the heat flux to the inner walls of the tube. The plasma gas (Q2) is introduced tangentially to stabilize the plasma discharge. The carrier (Q1) gas is injected at the centre of the torch through a high pressure water cooled stainless steel probe. It is through the probe that the powders are injected along with the carrier gas. There is an added stainless steel constriction at the tip of the torch which stabilizes the plasma and links the torch to the reactor chamber. All parts of the torch are water cooled for the exception of the quartz

confinement tube. The tube delays the mixing of the sheath and plasma gases to avoid overloading the plasma region due to the high flow rate of the sheath gas.

The flow rates of the gases fed to the torch are regulated and monitor through gas flow meters for both induction plasma installations.

4.1.2 Power Generators

In the first h.f. induction plasma installation shown in Figure 4.1, the high frequency generator of model TAFA 32*50 MC was build by Lepel. The maximum available power output is 50 kW and its oscillator operates at a frequency of 3 MHz. The maximum plate courant is of 12 A and the maximum plate potential is of 12 kV. The power for the installation is regulated by a simple rheostat.

For the second h.f. induction plasma installation seen in Figure 4.2, the high frequency generator of model T-100-3-KC-TL was also build by Lepel. As mentioned, its maximum power is of 100 kW and the oscillator operates at a frequency of 0.3 MHz. The plate courant is maintained below 15 A and the plate potential may approach 13 kV. The power to the plasma torch is also regulated by a simple rheostat.

4.1.3 Spheroidization Chambers

The dimensions of the two spheroidization chambers are not identical as seen in Figure 4.1 and Figure 4.2. However, they both have walls which are made of pairs of concentric water-cooled, stainless steel tubes. Both reaction chambers have connection which can be

adapted to the exit of the induction torch. The bottom of the chambers are used to collect the powders after they have been injected through the plasma. The presence of quartz windows in the chambers allows the operator to verify if the plasma is ignited and stable from the control panel of the power generator. Both reaction chambers are connected to the vacuum system and a powder collection system.

4.1.4 Powder Collection Systems

The laboratory is equipped with a vacuum pump which can be used for all the installations which require a vacuum. The installation seen in Figure 4.2 is simply connected to a cyclone for the collection of particles. The vacuum within the chamber is applied true the cyclone and therefore all exiting gases and powders flow into the cyclone where smaller particles can be collected.

The other induction plasma installation as seen in Figure 4.1 is also connected to a cyclone. However, the gases and the particles which escape the cyclone are then sent through two filters. The two filters are build of porous metal and can capture particles as fine as 5μm. The disadvantage to having filters after the cyclone is that since the vacuum is applied through the filters, the accumulation of fine particles on the filters increases the pressure drop accross the filter. After a certain operation period, the desired pressure in the chamber can no longer be maintained due to the particulate cake formed on the filters. The only material loss with this system is the particles which are smaller than 5μm and the material which remained in the vapour phase.

4.2 Powder Feeders

During all the experiments performed, a total of three different powder feeder were used. The necessity of having different powder feeder was due to the wide variety of powders and their different sizes. The powder feed rate required also determined which powder feeders could be used.

The first powder feeder was used for its high feed rate capacity and because some powders had a very large average diameter. The largest of particles where in the range of 250-300 μm. The powder feeder was a screw feeder with a screw of 16 mm diameter which did allow for a high feed rates. The exit size of the powder feeder also allowed for a powder injection by gravitation alone. This feature minimized the velocity of the powders and consequently increased their residence time in the plasma flame. The disadvantage to this powder feeder was that its total mass was above 30 kg without any powders and could not be easily emptied. This complicated the evaluation of the powder consumption. Calibration curves based on the rotational speed of the screw had to be completed prior to the experiments

The second powder feeder used was also a screw feeder. The diameter of the screw was 6.5 mm and therefore was preferred for fine powders. This powder feeder could also be easily emptied by tilting. This presented an easy way of determining the powder feed rates. The mass of powder in the powder feeder was simply weighed before and after each experiment consequently determining the amount of powder processed. A carrier gas had to be used to carry the powders pneumatically to the torch. Having a smaller screw did also reduce the maximum feed rate output therefore limiting the use of this powder feeder to low and medium feed rates.

The third powder feed rate used was a vibrating powder feeder. The amount of vibration would determined the resulting feed rate. The advantage of this powder feeder is that it could handle fine powders at very high feed rates. Therefore, this powder was used when the feed rates were to high for the small screw powder feeder. The vibrating feeder could also be weighed before and after experiments allowing for the determination of the powder feed rate. A carrier gas also had to be used to convey the powders to the torch.

4.3 **Analysis Techniques**

Many different equipment was used to perform various analysis of the original and resulting powders. The parameters which had to be determined were the particles average diameters, the composition of the powders, the resulting degree of spheroidization and a verification of the presence or absence of cavities within the processed powders.

4.3.1 Degree of Spheroidization

To obtain the degree of spheroidization of the resulting particles, image analysis was used. Initially, pictures of samples from the powders were taken. If the particles diameters were large enough, an optical microscope of model Metallux 3 manufactured by Leitz was used. If the optical microscope could not obtain clear pictures of the particles, an scanning electron microscope (SEM) of model JEOL JSM-840A was available. Once the pictures where obtained, they were analysed with an image analysis software. The Mocha software from Jandel Scientific was used. The spheroidization degree was evaluated on a numerical base rather than by mass percentage. The selection was done visually with two principal guidelines to confirm if particles where to be considered spherical. The first requirement was that the ratio of the shortest distance

through the particle to that of the longest distance through the particle be greater or equal to 0.9. A perfectly spherical particle would result in a ratio of 1. The second requirement was that no protruding peaks, sharp or smooth, had to be present. The presence of these peaks would confirm the incomplete melting of the particle since the surface tension of the liquid phase had not been the predominating shape determining factor. The amount of particles which were counted in each picture varied between 70 to over 500 depending on both the size of the particles and the magnification used. A minimum of two analysis was completed for each sample and an initial evaluation of the accuracy of the spheroidization evaluation procedure was completed. In this evaluation, four different pictures of samples were analysed and gave similar results therefore confirming that two analysis of the resulting powders would give satisfactory results.

4.3.2 Composition Analysis

The analysis of the composition is done to confirm the absence of phase change within the material or simply to confirm the absence of decomposition of the material. If either of these would be present, the energy equations used to estimate the heat flux to the particles would have to be modified for such cases. The method used to analyse the compositions and phase compositions of the original powders versus the powders after r.f. induction plasma treatment was X-ray diffraction. An X-ray diffraction apparatus of model Rigaku Giegerflex was used for the analysis. Once the analysis are done, key peeks within the spectrum are compared amplitude wise to verify that no changes in the powders occurred during the powder treatment.

4.3.3 Porosity Analysis

An analysis of the porosity of the resulting powder was done to verify if any cavities were present within the individual molten particulates. The powders are first embedded in an epofix resine from Struers. Once the resign has hardened, the cylinder containing the powders is polished with a grinder-polisher from Buehler. The initial polishing cuts the powders to obtain cross sections of the spheres. Final stages of polishing reduce the surface to a smooth and uniform plane. Once the sample preparation has been completed, they are analysed by optical microscope to verify the presence or absence of cavities within the treated powder.

4.3.4 Particle Size Distribution

The determination of the mean diameter and size distribution of both the original and resulting powders had to be determined. This information is necessary first to compare the diameters and distribution of the powders for obvious evaporation of matter or agglomeration of particles. Both options are not desired during the experimental study. Secondly, the mean diameter of the particles is a parameter of critical importance in the estimation of the heat transfer from the plasma to the particles.

To obtain the mean diameter and distribution of the powders which were known to be smaller than 100 μm, a sedigraph of model Sedigraph 5000ET from Micromeritics was used. A cumulative probability graphic is the output which identifies the mean diameter of the particles inserted and their distribution.

For the larger powders, standard sieves where used to determine both the mean diameter and the distribution of the particles. The powders were processed following the standard ASTM guidelines to obtain the desired information.

4.4 Operating Conditions

The thermophysical properties used for the various powders used along with all the operating conditions for the individual experiments are presented next since both are crucial in determining the parameters of the model and also of ensure the reproduction of the results.

4.4.1 Thermophysical Properties of the Powders

In all the experiments performed for the research, a total of five different materials were used. Among this variety, there was also a large range of mean diameters. The list of the powders and the dimensions used are presented in Table 4.1.

TABLE 4.1 THERMOPHYSICAL PROPERTIES OF THE POWDERS

Powder	ρ kg/m^3	k W/(m*K)	C_p J/(kg*K)	T_m K	λ_m MJ/kg	T_v K	D_p, σ_p μm
Al_2O_3	3810	6.28	810.3	2325	1.07	3253	45, 11
Cr_2O_3	4930	12.5	790	2607	0.12	3270	27, 5
SiO_2	2650	1.3	743	1986	0.24	2503	99-196
ZrO_2	5490	1.5	455.8	2973	0.71	5273	52, 22
WC	15630	121	180.4	3140		6273	197, 21

4.4.2 Plasma Operating Conditions

A wide variety of plasma operating conditions were also used. The reason for the choice of plasma gases was to avoid the reaction of the powders with the gases. This would have introduced another change in the particles such to complicate the prediction of the process efficiency. Some other parameters of the process were also varied to identify preferential operating conditions as the pressure or power. There was also a consideration of the economic aspect of the process. For example, air was used in large quantities where possible as to minimized the cost of the eventual process. So the conditions used that have not already been identified earlier are presented in Table 4.2.

TABLE 4.2 EXPERIMENTAL OPERATING CONDITIONS

Set	Powder	Power kW	f MHz	P kPa	Sheath slpm	Central slpm	Carrier slpm	D_p, σ_p μm	Range of feed rate g/min
1	WC	80	0.3	33	100/24-Ar/H_2	30-Ar	1-Ar	197, 21	47-149
2	WC	80	0.3	67	100/24-Ar/H_2	30-Ar	1-Ar	197, 21	50-100
3	SiO_2	80	0.3	93	120-air	30-Ar	1-Ar	177, 18	18-51
4	SiO_2	100	0.3	93	120-air	30-Ar	1-Ar	177, 18	18-50
5	SiO_2	50	3	73	100-air	30-air	5-Ar	177, 18	26-89
6	SiO_2	50	3*	53	90-air	27-Ar	8-Ar	99-196	10.5-124.8
7	SiO_2	50	3	101	90-air	16/16-air/Ar	8-air	177, 18	33.2-383
8	Al_2O_3	50	3	101	90-air	16/16-air/Ar	8-air	45, 11	26.5-456
9	Cr_2O_3	50	3	101	90-air	16/16-air/Ar	8-air	27, 5	12.2-84.3
10	ZrO_2	50	3	101	90-air	16/16-air/Ar	8-air	52, 22	12.7-120

* The coil of the torch had 5 turns compared to the usual 4 turns for the 3 MHz installation.

CHAPTER 5

RESULTS AND ANALYSIS

The results of the experiments are presented in a defined order. The actual spheroidization and efficiency results are presented followed by a verification of the assumptions made prior to the experiments. The presentation of the resulting models and the evaluation of their performances conclude the chapter.

5.1 Spheroidization Efficiency

Once the powders treated, they were analyzed optically to determined their spheroidization percentage. These results are number based percentages. A sample of each powders is shown in Figure 5.1 through Figure 5.10 in their initial condition compared to a sample of the resulting powder from a particular experiment. From the photographs of the original powders, we can see that in addition to the parameters taken into account, there is a large variety of original powder shapes. In particular, if Figure 5.3 is observed, we notice that the original powders already had a rough spherical shape. The shape aspect of the particles is another variable which could affect the performance of the model as the heat transfer in the actual particles is not exactly similar to that of a sphere.

5.2 Densification of the Particles

Plasma treatment of powders has been known to be used for the densification of powders. However, as shown in section 2.7, due to the difference of density between the liquid phase and the solid phase, there is a possibility of the creation of cavities within the particles. Many

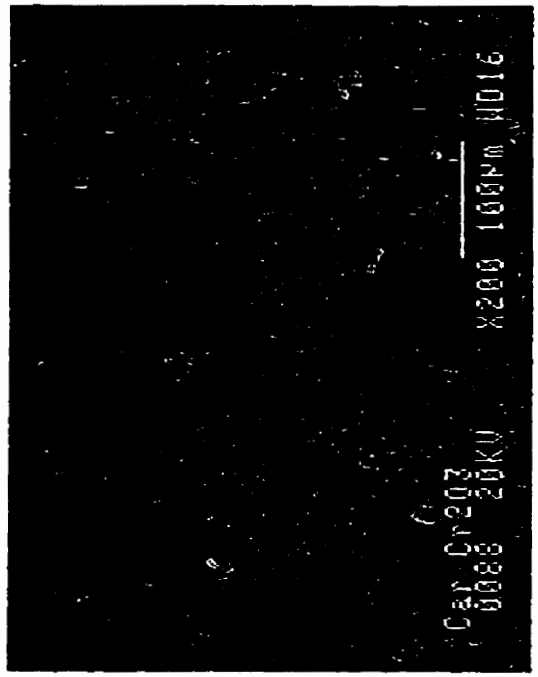

Figure 5.1 Original chromium oxide powders

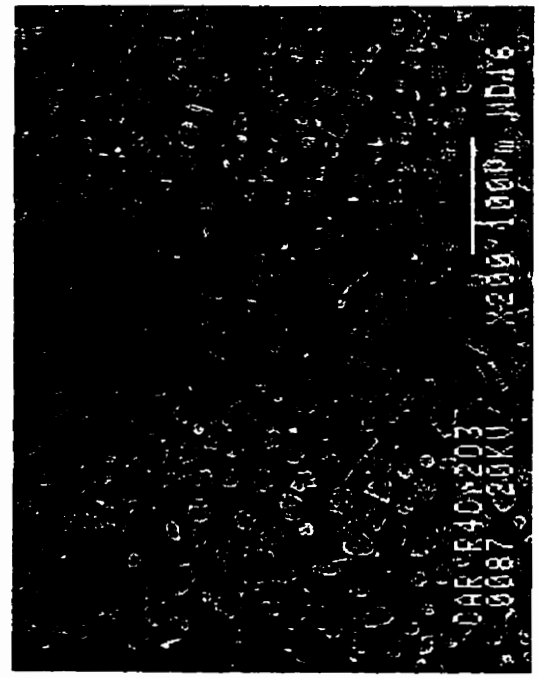

Figure 5.2 Chromium oxide treated powders (22.7g/min;50kW; 101kPa)

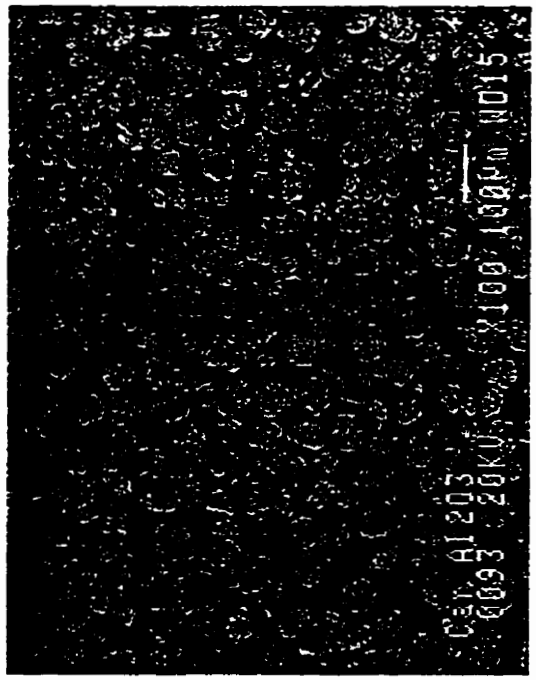

Figure 5.3 Original alumina powders

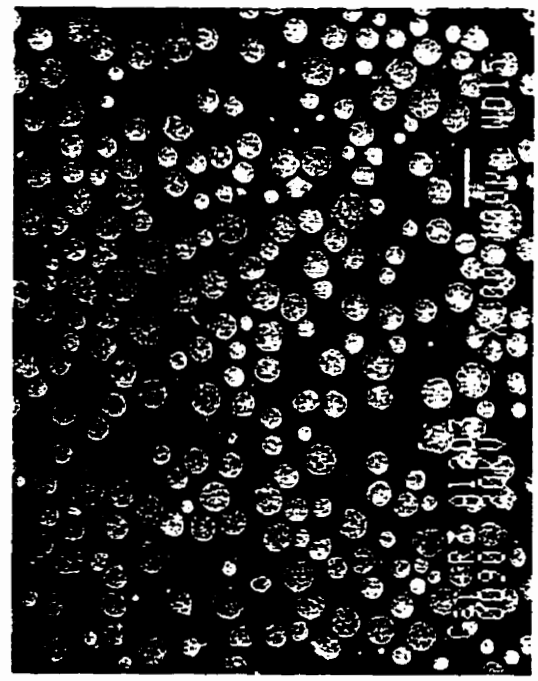

Figure 5.4 Alumina treated powders (26.5g/min;50kW;101kPa)

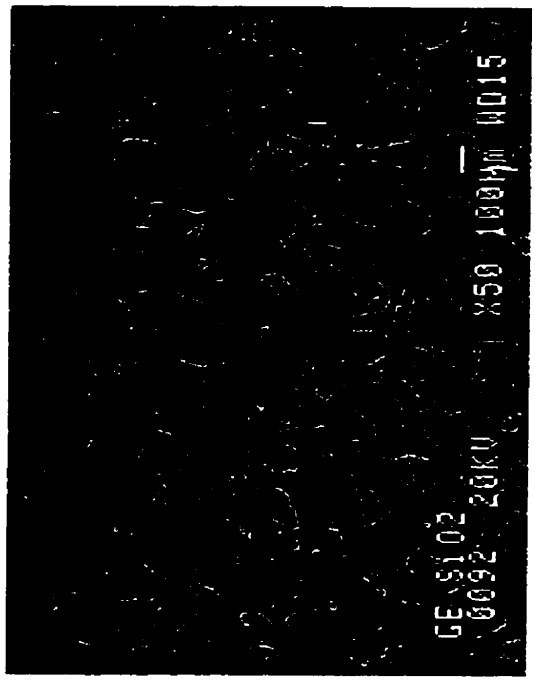

Figure 5.5 Original silica powders

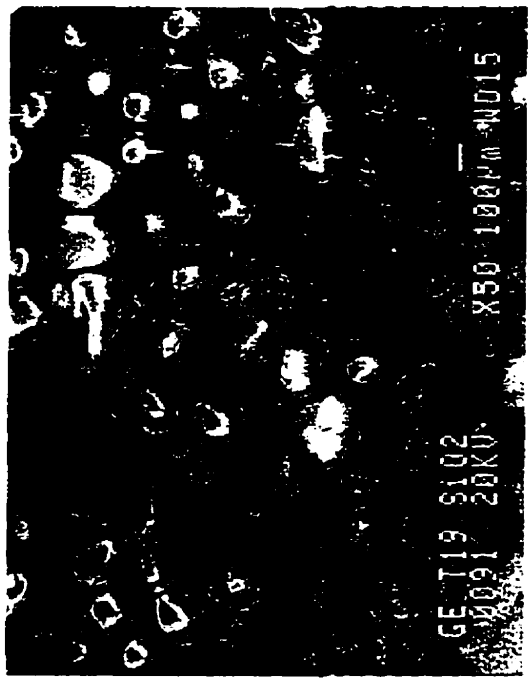

Figure 5.6 Silica treated powders (54g/min;50kW;73kPa)

Figure 5.7 Original tungsten carbide powders

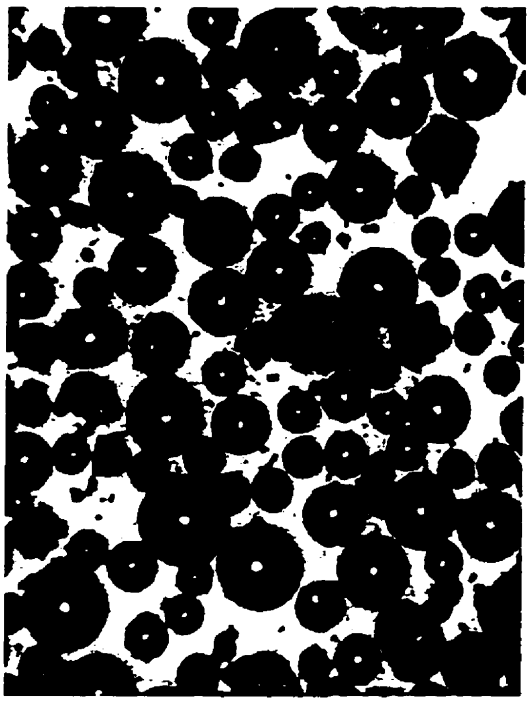

Figure 5.8 Tungsten carbide treated powders (50g/min;80kW; 0.3MHz;67kPa)

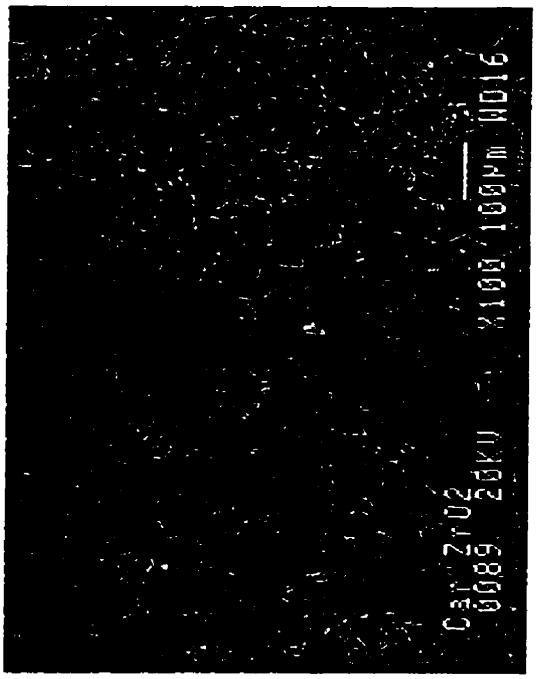

Figure 5.9 Original zirconia powders

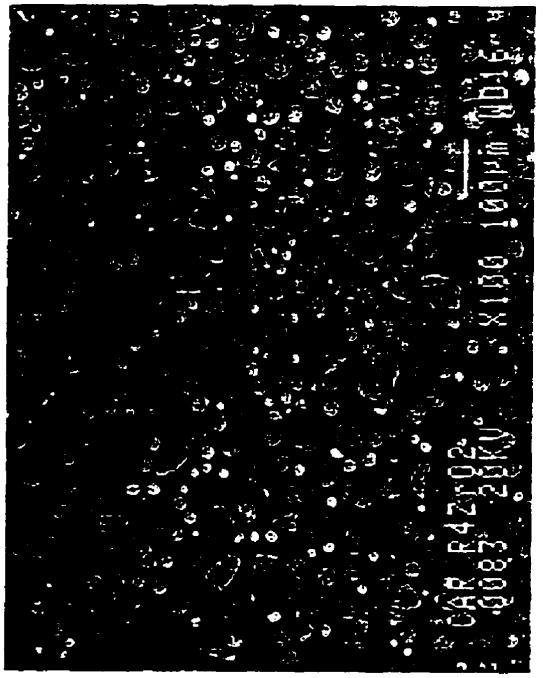

Figure 5.10 Zirconia treated powders (28.6g/min;50kW;101kPa)

parameters can affect this result as the actual difference in densities of the material and the rate of the quenching.

The difference in densities between the liquid and solid phase can not be controlled and varies form one material to another. However the rate of the quenching, if wanted, can be controlled. The estimation of the radius of the resulting cavities presented by Equation 2-4 does not take into account the rate of quenching. It is however an important variable in the possible presence of cavities within the resulting particles. If the quenching is rapid, as is the case in most plasma processes, the outer shell of the particles will solidify while the center remains in the liquid phase and at a lower density. The diameter of the shell is therefore directly dependent on the rate of quenching which in turn depends on the temperature gradient. The temperature

gradient is a function of the thermal conductivity of the particles and other thermal properties as the specific heat capacity. If small particles are treated, there is a smaller volume of the liquid phase remaining in the inner shell and therefore if a cavity is formed, it will in turn be smaller. So by treating particles of large diameters, an enlargement of the particles could be observed.

To evaluate these possibilities, the silica and tungsten carbide powders which had larger mean diameter where analyzed. The resulting powders were cemented in a resin and then cut in half to observe if any cavities were present. This was also done with the original tungsten carbide powders to demonstrate that no cavities were present initially and that the cavities are a result of the heat treatment. The absence of cavities in the original powders is shown in Figure 5.11. However, as shown in Figure 5.12 and Figure 5.13, there are large cavities present in the plasma processed particles. To further the investigation, an analysis of the mean diameter of the resulting powders was also completed to determine if it had increased. There was however conflicting results. The average mean diameter of the tungsten carbide had indeed increased by 4 μm while the average mean diameter of the silica powders had actually decreased by 2 μm. These results might initially seem not possible but as discussed in section 5.2, the evaporation of some material has for consequence to reduce the average mean diameter of the particles. It remains to see in particular cases which phenomenon while dominate over the other and it could eventually be defined at which conditions these will equal each other. These results prove that an initial distribution analysis of treated powders can not in itself determined what has occurred to the particles during the heat treatment of these.

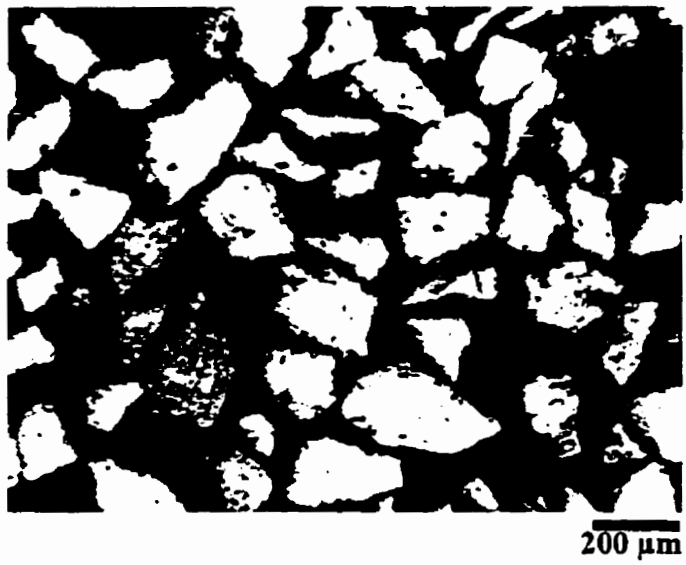

Figure 5.11 Picture of a cross section of the original cut tungsten carbide powders

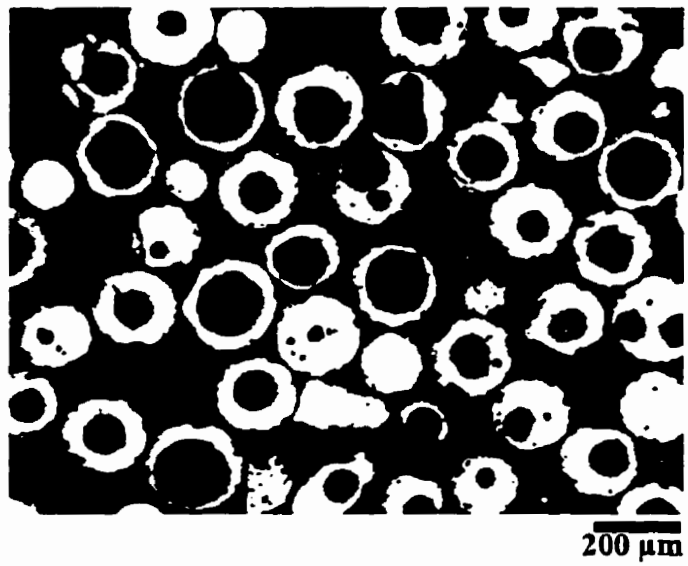

Figure 5.12 Picture of a cross section of the cut tungsten carbide powders after being treated by induction plasma

Figure 5.13 Picture of a cross section of the cut silica powders after being treated by induction plasma

5.3 **Minimal Evaporation of the Particles**

The assumption that there is a minimal evaporation of the particles was done since it is justified at the optimal operating conditions. The optimal conditions were wanted and it is at these conditions that the temperature gradient within the particle is the smallest while retaining the melting of the particles.

It is known that there is however some evaporation of material and the quantity of evaporation is dependent (aside the melting and evaporation temperatures) on the thermal conductivity of the material. It is therefore different for every material. It has previously been shown however by [ISHIGAKI, 1991] that the evaporation of some of the particles will simply have as an effect to reduce the mean diameter of the resulting plasma treated powders. This later

observation is however not always true due to other phenomenons which occur during the quenching of the particles as will be shown in section 5.3.

So even though we know that the assumption of having no evaporation present is not accurate, it is either small at the optimal condition or can be reflected in the semi-empirical model by the presence of the melting temperature, the evaporation temperature and the thermal conductivity of the powders involved in the process.

5.4 Absence of Reactions

One of the most important assumptions which was assumed is that the powders do not react or decompose during their plasma processing. This assumption was done such that the heat treatment of the particles would be the only factor which would have to be taken into account and therefore be studied. To ensure the validity of assuming the absence of reactions between the particles and the surrounding gases, the gases used in the particular experiments where chosen in accordance with the reactive nature of the materials. As such, air or oxygen was used with oxides and hydrogen was used with the tungsten carbide to avoid the oxidation of the tungsten.

Once these precaution were taken, the analysis of the original and resulting powders was done to evaluate if there was any degradation of the raw powders or the formation of new species. The result of the X-ray diffraction analysis are presented graphically in Figure 5.14 through Figure 5.23. They include all five different powders used during the experiments. As it can be seen from Figure 5.14 and Figure 5.15, the zirconium oxide was originally composed of the baddeleyite (monoclinic) zirconium dioxide phase. It is also the case for the treated zirconium

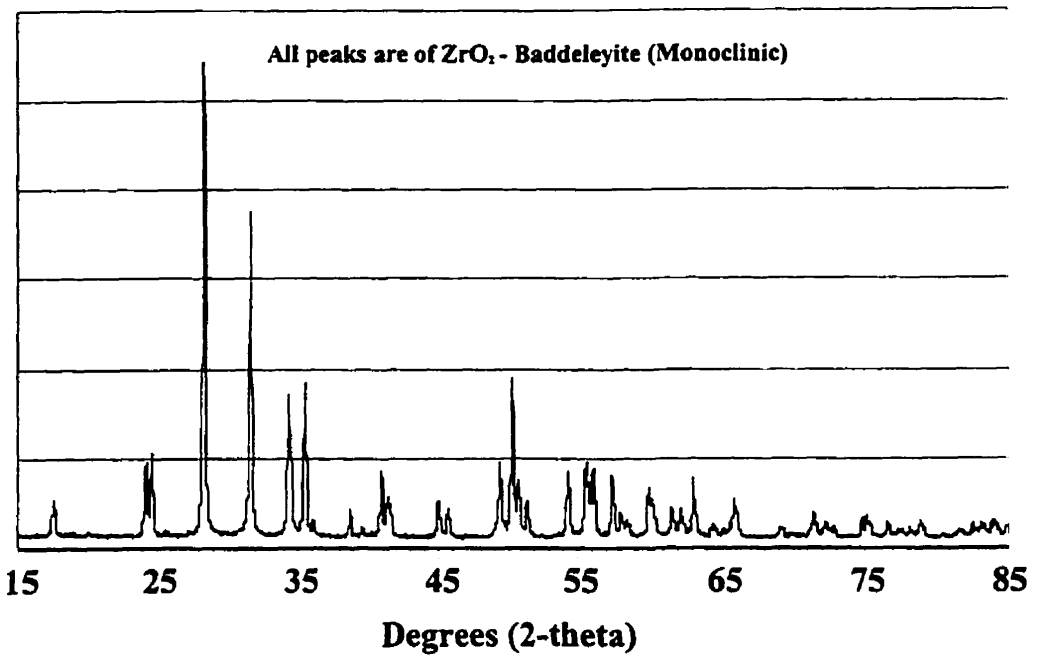

Figure 5.14 X-ray diffraction analysis of the original zirconium oxide powders

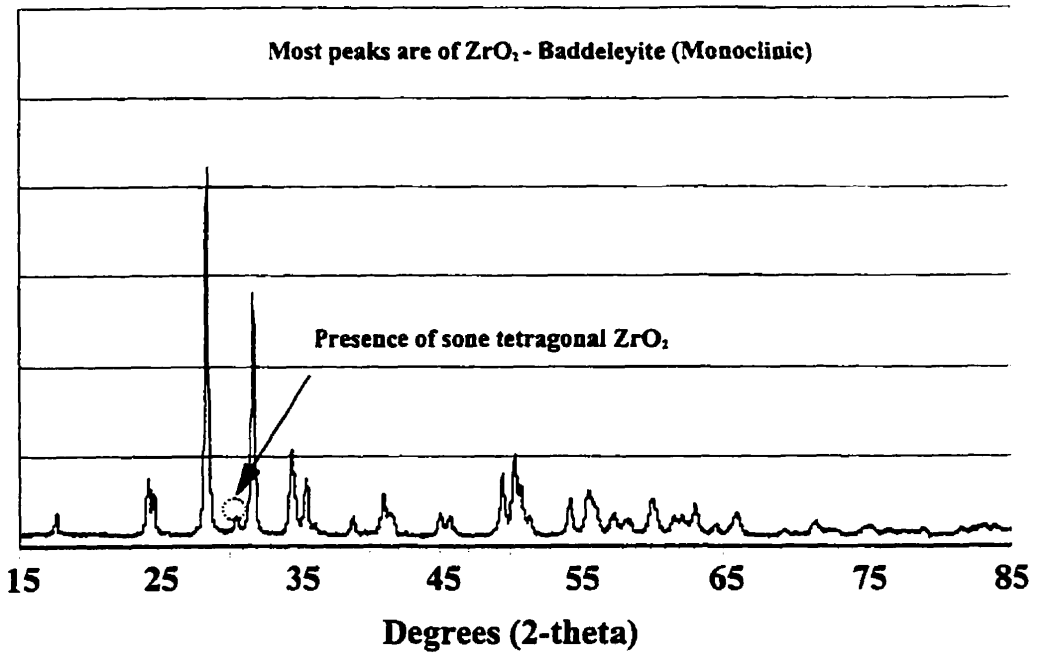

Figure 5.15 X-ray diffraction analysis of the plasma treated zirconium oxide powders

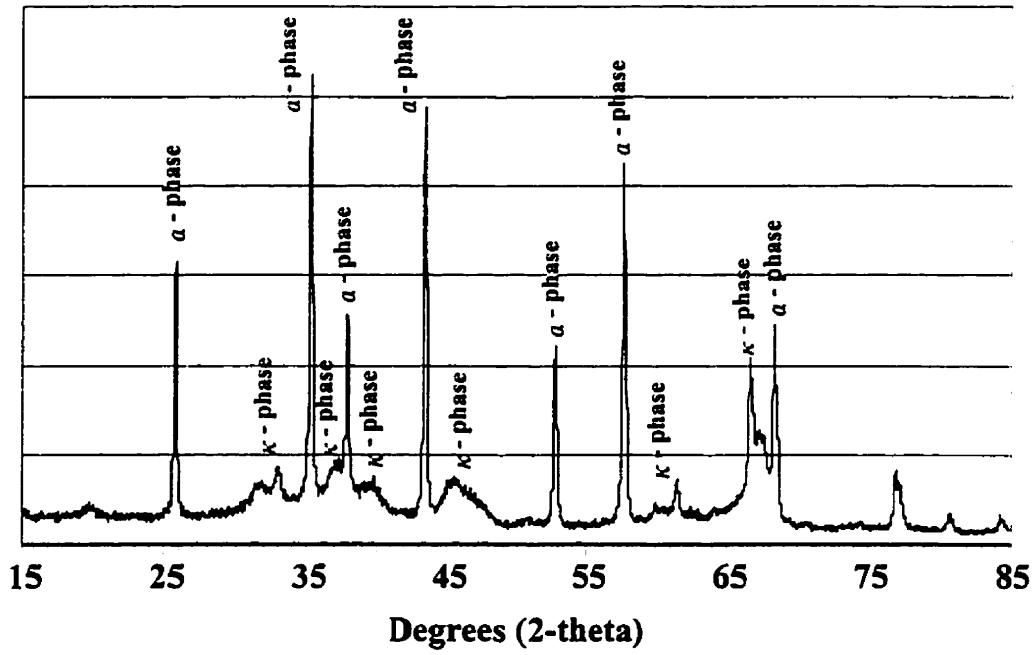

Figure 5.16 X-ray diffraction analysis of the original aluminum oxide powders

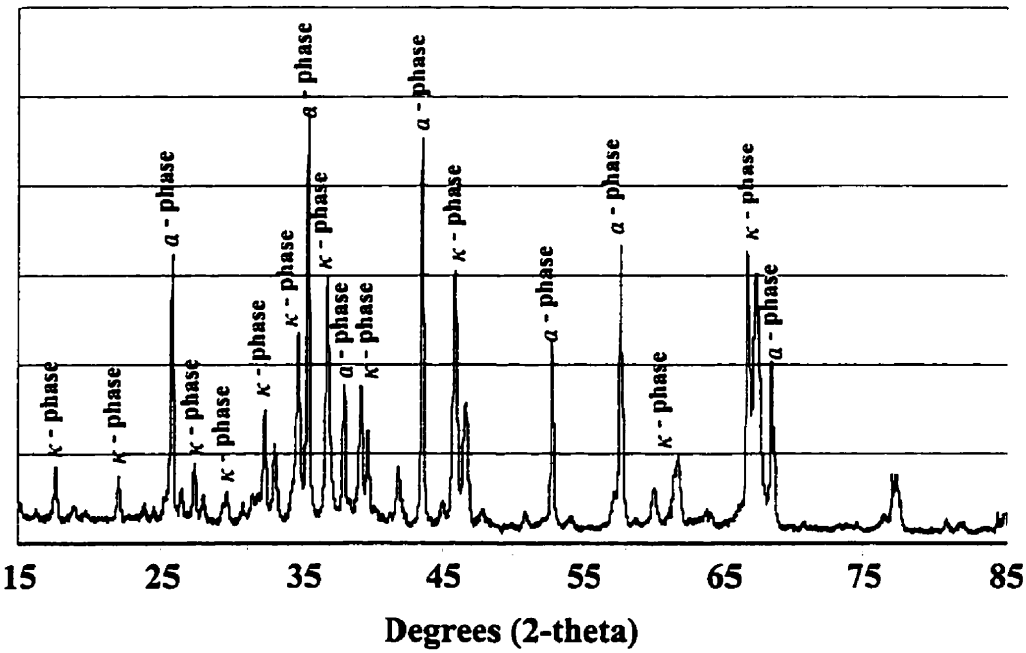

Figure 5.17 X-ray diffraction analysis of the plasma treated aluminum oxide powders

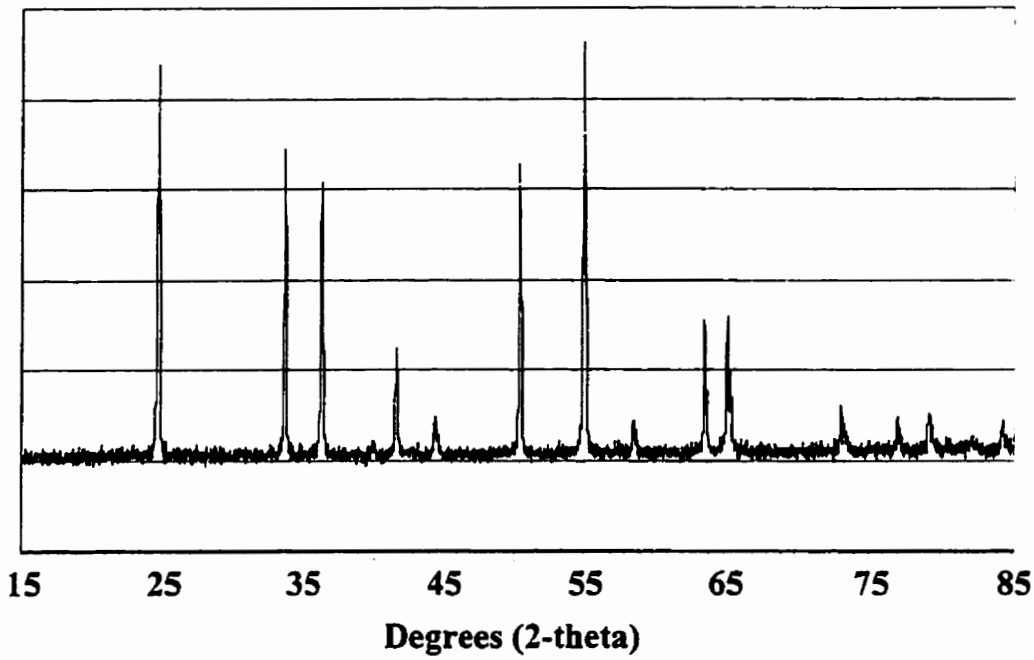

Figure 5.18 X-ray diffraction analysis of the original chromium oxide powders

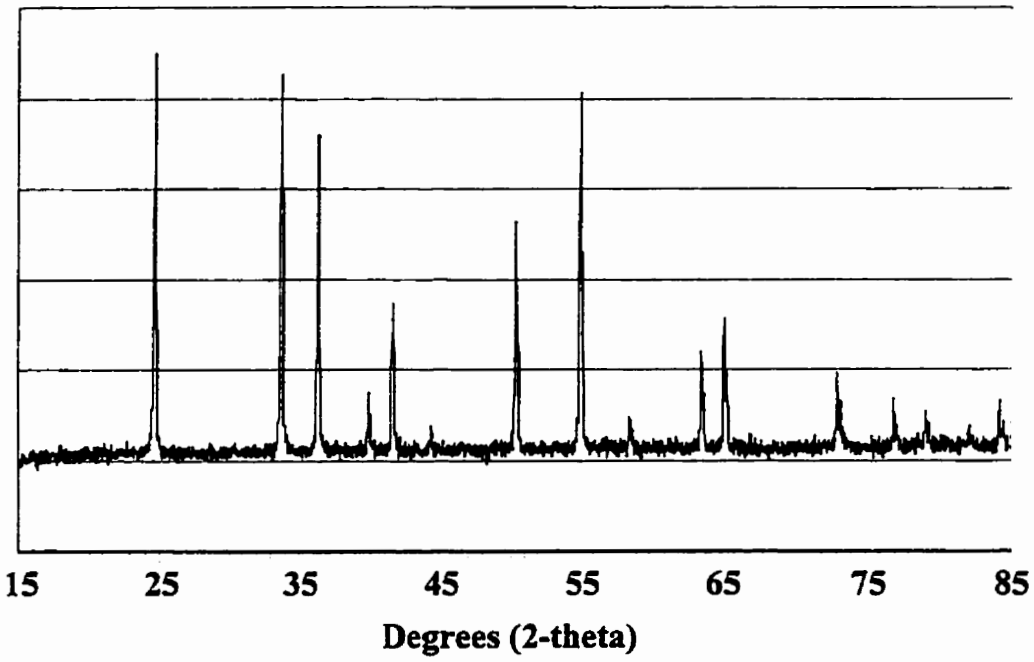

Figure 5.19 X-ray diffraction analysis of the plasma treated chromium oxide powders

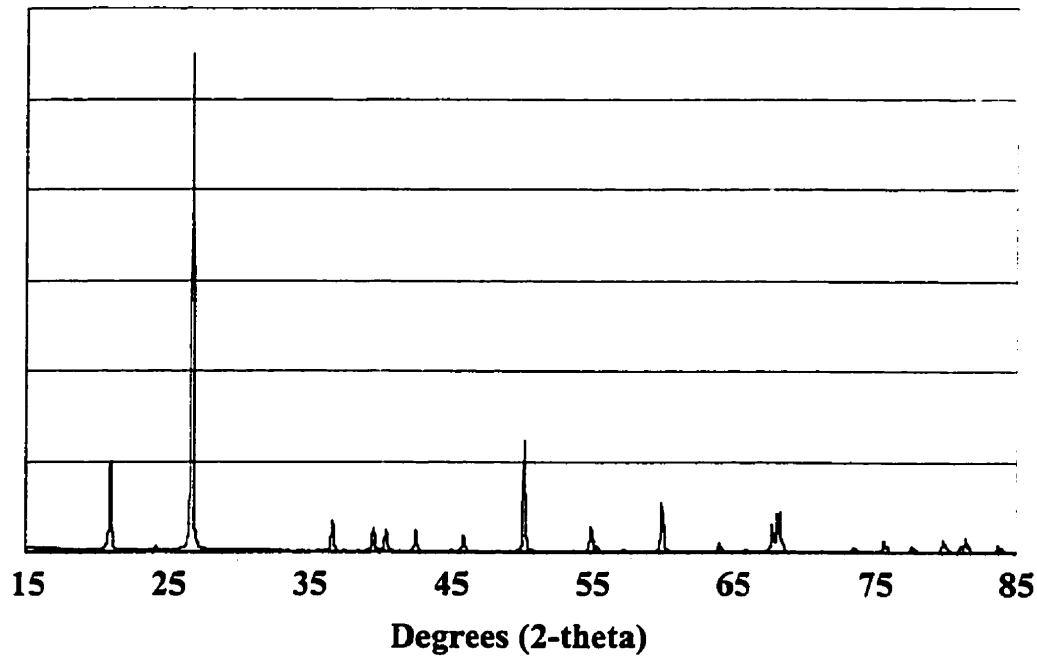

Figure 5.20 X-ray diffraction analysis of the original silica powders

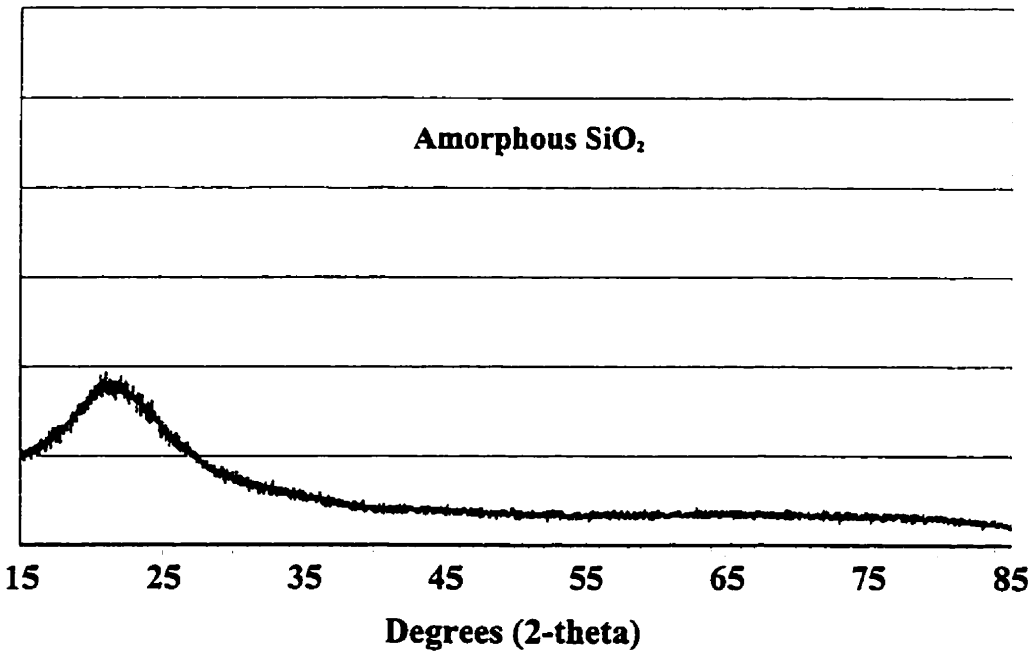

Figure 5.21 X-ray diffraction analysis of the plasma treated silica powders with the amplitude scaled up ten folds relative to the original powders X-ray analysis

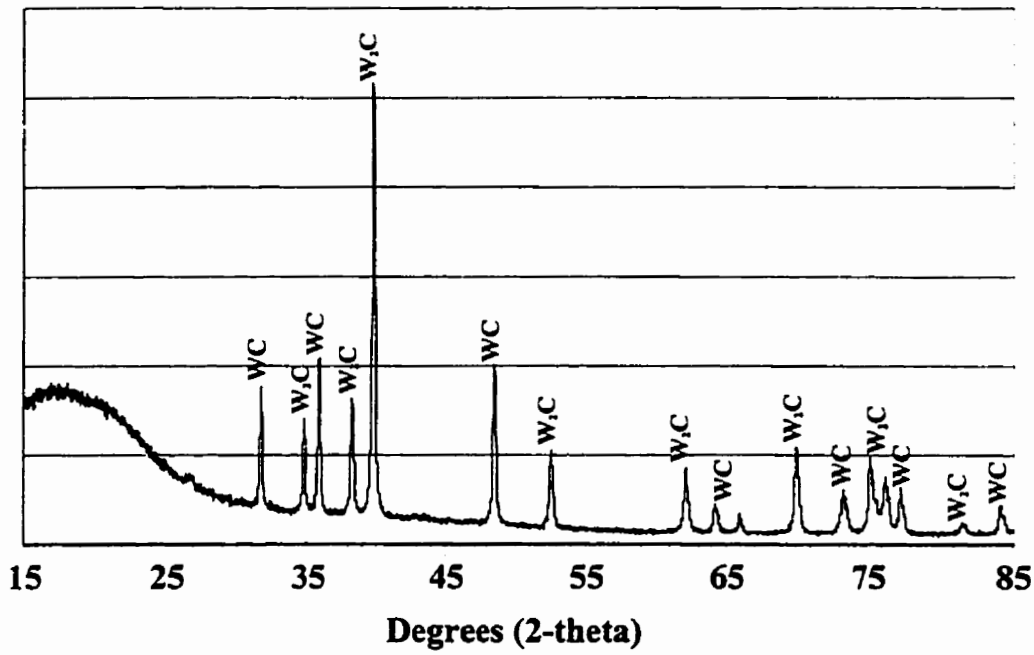

Figure 5.22 X-ray diffraction analysis of the original tungsten carbide powders

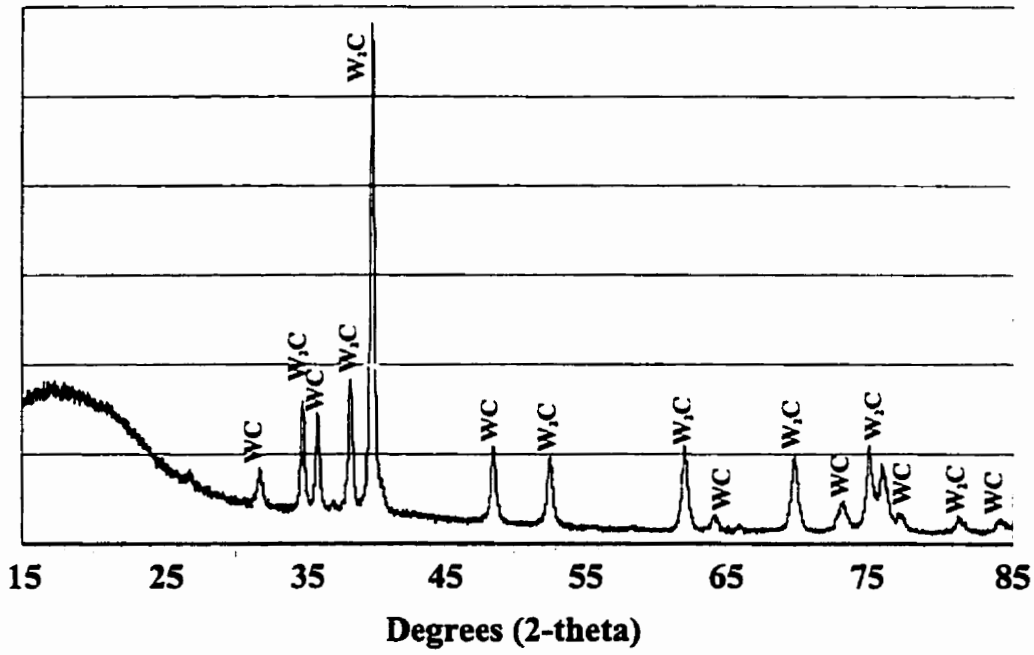

Figure 5.23 X-ray diffraction analysis of the plasma treated tungsten carbide powders

oxide powders with the exception of the slight presence of the tetragonal form of zirconium dioxide as it is identified by the arrow in Figure 5.15. The treated powders were processed with the conditions of the experimental set #10 with a powder feed rate of 28.6 g/min. The X-ray analysis were generally performed with experiments of lower feed rates such that if any reactions were to occur they would be present since the probability of them occurring at low feed rate is greater. So we can therefore assume that there is no significant change in the composition of the zirconium oxide powders specially due to the absence of any zirconium metal.

By observing Figure 5.16, we can determine that the original aluminum oxide powders were mainly composed of the corundum phase also known as the α-phase. This is the natural mineral form of aluminum oxide. We most notice however that there is also a small presence of the κ-phase. The treated powders which were analyzed in Figure 5.17 were processed under the conditions of the experimental set #8 with a powder feed rate of 33.7 g/min. As shown in the figure, there is a much greater presence of the κ-phase at the expense of the α-phase. However, there is no presence of aluminum metal or of the free form of aluminum oxide in the treated powders. In this case, there is a change in the composition of the resulting powders or more specifically in there final state.

The analysis of the original chromium oxide powders shown in Figure 5.18 determines that the powders were eskolaite chromium oxide which is under the form Cr_2O_3. The treated powders which are analyzed in Figure 5.19 were processed under the conditions of the experimental set #9 with a powder feed rate of 22.7 g/min. As it can be seen with Figure 5.18,

they are identical which means that there were none of the other forms of chromium oxide formed and that no decomposition into the chromium metal occurred either. So for the chromium oxide, the assumption of the absence of reactions was accurate.

Figure 5.20 is the X-ray analysis of the original silica powders. The original powders were silica in the quartz form. No other forms of silica were present. However, as it can be seen in Figure 5.21, the plasma treated powders with the conditions of the experimental set #5 and a feed rate of 54 g/min are amorphous. None of the particles had the required time during the quenching section of the process to recrystalize. There is however no signs of free silicon in the resulting powders. For the silicon particles, there is no reactions but the final state of the crystalline structures are not the same as the original powders.

The last original powders to be analyzed are the tungsten carbide powders. In this case as shown in Figure 5.22, two different structures of the compound are initially present. There is a larger proportion of tungsten carbide in the W_2C form compared to the WC structure. The treated powders which were analyzed in Figure 5.23 were obtain with the conditions of the experimental set #1 and with a feed rate of 100 g/min. In the X-ray analysis, we can observe that both original structures are still present. However, as shown in the figure, there is much less tungsten carbide in the WC form and a greater proportion in the W_2C form. There is on the other hand no presence of a decomposition into tungsten metal or other structure of the compound. So for the case of the tungsten carbide powders, there a significant change of structure within the microscopic composition of the powders which does affect the initial assumption which expected no reactions in the particles other than the heat treatment and therefore shape modification.

The powders which did have some phase changes can be justified by the thermodynamic equilibrium of these. The phases of the material which are favored at high temperature are predominant in the resulting powders due to the quick quenching. The high temperature phase does not have the required time to return to the low temperature favored phase. This can be shown with the tungsten carbide powders in Figure 5.24. Figure 5.24 is the thermodynamic equilibrium diagram for a C-H-W system. As it can be seen, the W_2C phase is more stable at high temperature than the WC phase and explains why more of the first phase is obtained in the resulting powders.

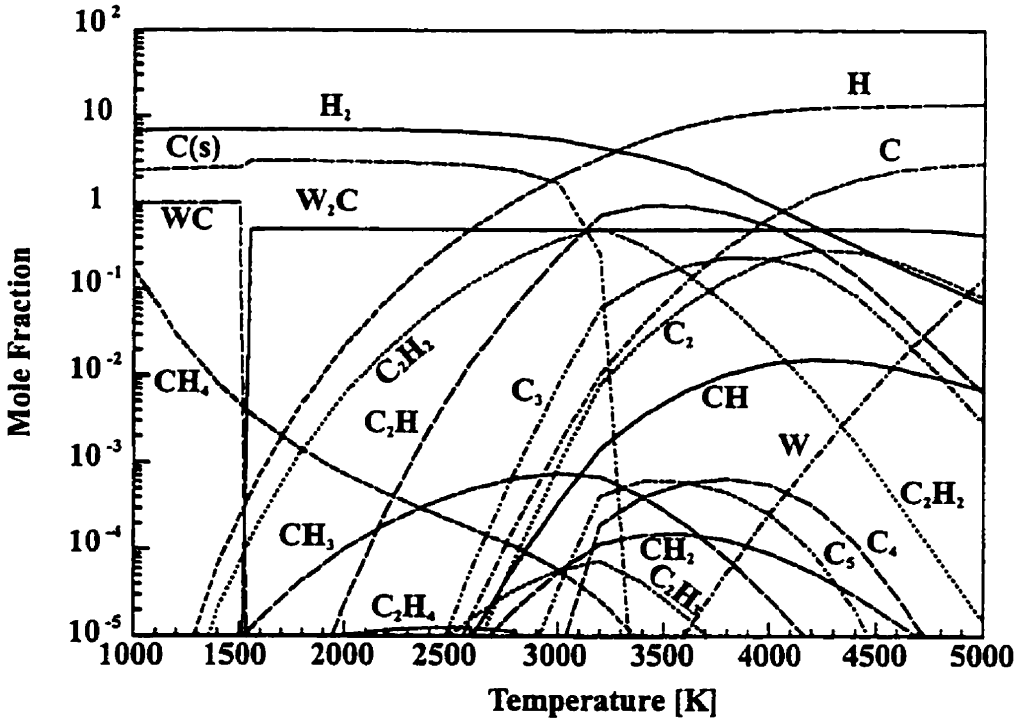

Figure 5.24 Thermodynamic equilibrium diagram of a C-H-W system demonstrating the preference of the W_2C phase to the WC phase at high temperatures (above 1500 K)

5.5 Theoretical Energy Efficiency

To determine the value of the unknown parameter (Z) in Equation 3-4, the energy efficiency of the experiments must be determined as a function of the feed rate. With the earlier assumption which assumes minimal evaporation of the particles, the energy absorbed can be determined and later compared to the power which was fed to the process during the plasma induction of the particles. The result for the experimental set #3 through set #5 and set #7 through set #10 are presented in Figure 5.25 and Figure 5.26 respectively. As it can be seen in Figure 5.25, there is a greater power efficiency for set #5 which was processed with the higher frequency system and with a power input of only 50 kW. By comparing set #3 and set #4, there is an increase in the energy efficiency when the power input is increased for given feed rates. It must be noted that for all three cases however, the feed rates are relatively low and there is no maximum apparent. So for all three cases, it is therefore not possible to obtain an estimation of Z for Equation 3-4.

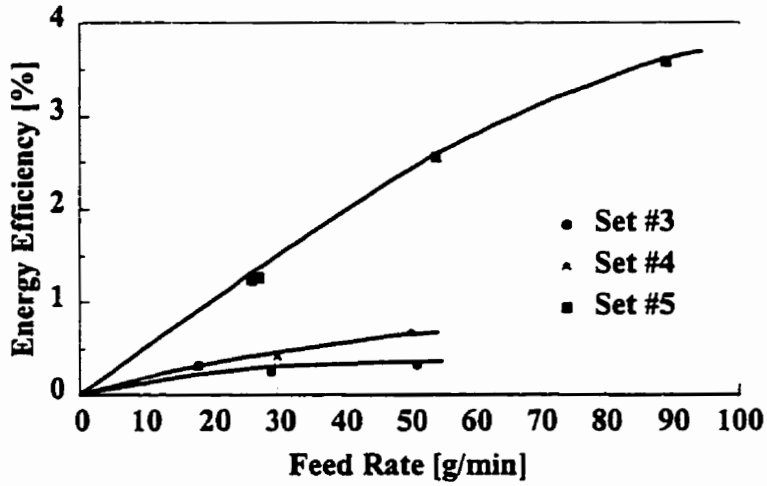

Figure 5.25 Energy efficiency of set #3; 80 kW, 0.3 MHz, set #4; 100 kW, 0.3 MHz and set #5; 50 kW, 3 MHz, all being SiO_2 powders

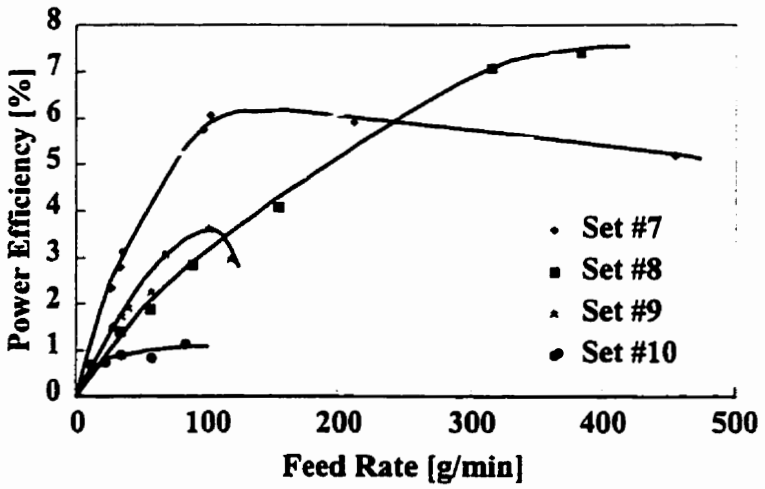

Figure 5.26 Energy efficiency of set #7; SiO_2, set #8; Al_2O_3, set #9; Cr_2O_3 and set #10; ZrO_2, all with identical operating conditions of 50 kW and 3 MHz

When observing Figure 5.26, there are for these sets of experiments, apparent maximums in the energy efficiency of the systems. All four sets can be directly compared since their operating conditions were identical. The difference in the energy efficiency behavior of the curves is therefore directly related to thermophysical properties of the powders and their interactions with the plasma. The energy efficiency behavior does reflect what was predicted by [PROULX, 1987]. However, in the present case, higher feed rates were used which revealed a diminution of the efficiency after reaching its maximum. So the determination of Z for these sets of experiments is simply a estimation of the maximum energy which can be absorbed by the particles from the total power input. The resulting values for the parameter Z in Equation 3-4 are presented in Table 5.1.

TABLE 5.1 VALUES OF THE *Z* PARAMETER

	Set #7	Set #8	Set #9	Set #10
Z	0.675	0.550	0.104	0.328

As it can be seen, since the values of *Z* are near unity, the previous choice of 0.11 as the average total energy absorbed by the particle from the plasma was justified. The reduction in the energy absorbed can also be observed when using the results of Equation 3-4 to predict the spheroidization efficiency of the powders beyond the maximum. Figure 5.27 represent the predicted curves of the model and it can be seen that the actual experimental points of set #8 and set #10, which are beyond the critical maximum, are slightly lower than predicted. The other inconvenient to the model is that it is not useful prior to the critical point. That is however the region of preferred operation as the resulting spheroidization efficiencies are higher.

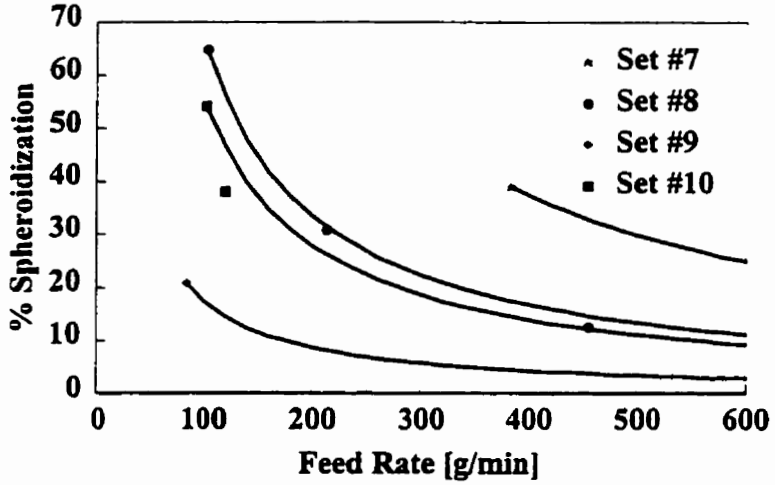

Figure 5.27 Spheroidization efficiency of the model and the actual experimental results

5.6 Empirical Models

The empirical model from equation 3-5 has three parameters which are to be determined experimentally for sets of powders. This model is useful for the processes that continually use the same powders which is the case for regular industrial applications. Since the characteristics of the system and of the powders remain the same, once the parameters of the model are obtained, the model can be used to determine the efficiency for the desired feed rate. It can also be used with powders for which some thermophysical properties are not be available. The values of the parameters for the model are presented in Table 5.2 for set #1 through set #5 and set #7 through set #10.

TABLE 5.2 VALUES FOR THE PARAMETERS OF THE EMPIRICAL MODEL

	Set #1	Set #2	Set #3	Set #4	Set #5	Set #7	Set #8	Set #9	Set #10
Powders	WC	WC	SiO_2	SiO_2	SiO_2	SiO_2	Al_2O_3	Cr_2O_3	ZrO_2
θ_0	86.5	88.5	100	100	100	100	100	100	84.9
ω	0.0031	0.0060	0.0636	0.2286	0.0038	0.0484	0.0086	0.0549	0.0078
n	1.5	0.323	0.713	0.132	1.5	0.155	0.775	0.589	1.115

The resulting spheroidization efficiencies are presented for the sets of experimental data in Figure 5.28 and Figure 5.29. The first figure containing the sets of data which were completed with the 0.3 MHz installation while the second figure includes the sets completed with the 3 MHz installation.

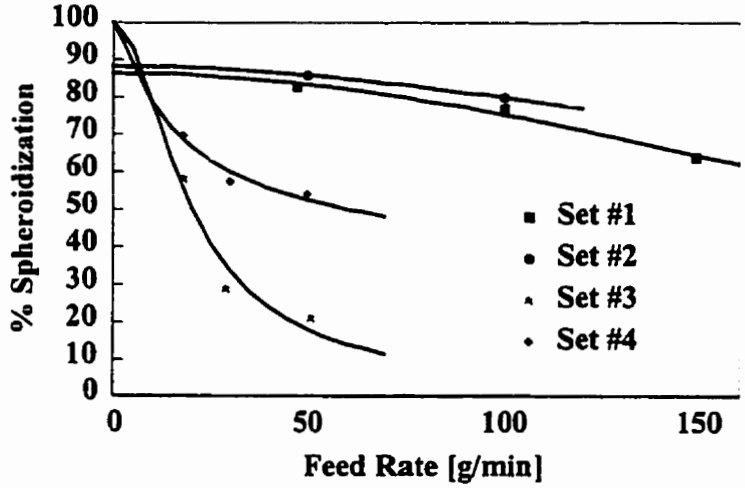

Figure 5.28 Spheroidization efficiency as predicted by the empirical model for set #1 through set #4

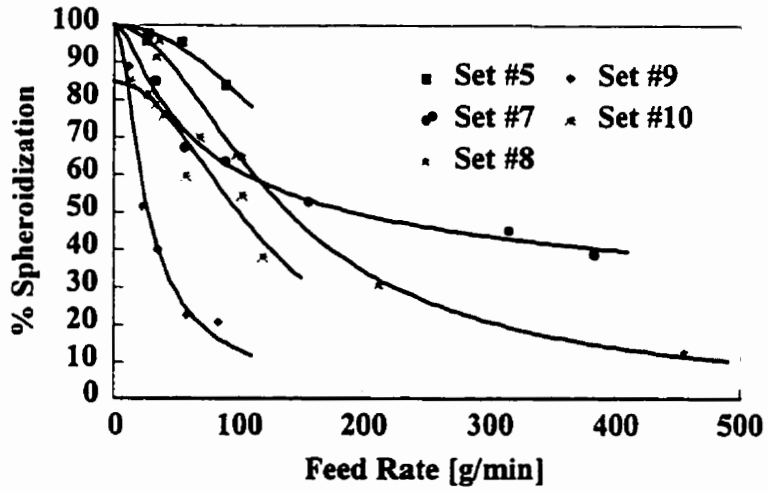

Figure 5.29 Spheroidization efficiency as predicted by the empirical model for set #5 and set #7 through set #10

As mentioned in section 3.3, the next step is to introduce a semi-empirical model which takes into account the effects due to the change in diameter, the only thermophysical property of the powders which can be isolated. The semi-empirical model presented in Equation 3-6 contains a function Ψ_X which represents the relation between the earlier model and the mean diameter of

the particles. The model will be useful for the same cases as the earlier model except that if changes in the size of the powder occur due to the manufacturer, a correction of the operating feed rate will be possible with the model. Silica particles of mean diameter 99, 139 and 196 μm were taken an treated with identical induction plasma conditions to compare the effects of the change in mean diameter. After optimizing the model with the resulting data, values for the six parameters were obtained. The three parameters of the empirical model are not accurate since the new parameters no longer include the effect of the diameter. The values of the new parameters are presented in Table 5.3.

TABLE 5.3 PARAMETERS OF THE DIAMETER BASED SEMI-EMPIRICAL MODEL

Parameter	Value	Parameter	Value
θ_d	0.490	Ψ_1	-0.5607
ω_d	0.5079	Ψ_2	0.7457
n_d	1.641	Ψ_3	-0.4804

The prediction of this model is represented in Figure 5.30. It represents the predicted spheroidization efficiency for the silica powder of the previously mentioned mean diameters along with the experimental data. It can be seen that the model sufficiently represent the spheroidization efficiency of the powders specially in the range of high spheroidization efficiency. It must be noted that in this case, there is some discrepancies in the experimental data since for certain feed rates, the spheroidization efficiency of the smaller particles is lower than that of the larger particle which is theoretically not possible.

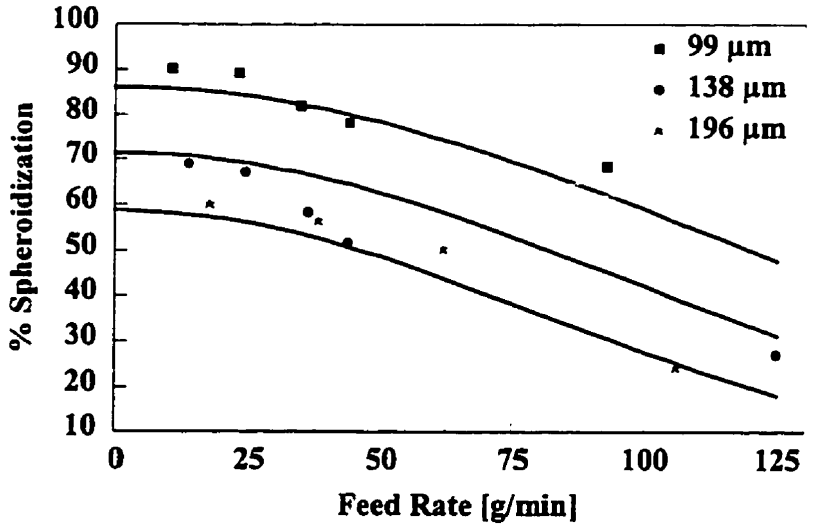

Figure 5.30 Spheroidization efficiency as predicted by the diameter based semi-empirical model for silica powder with experimental conditions of set #6

The last step to developing the model is determining the thermophysical property based semi-empirical model. Since the diameter effect has been isolated, it is now possible to isolate the other thermophysical properties by keeping the induction plasma operating conditions identical for various sets of experiments. This was done with set #7 through set #10 which include a total of four different powders, silica, alumina, chromium oxide and zirconia. The resulting model however is quite complex as it was shown in Equation 3-7. It follows that the optimization of the parameters for the model was also complex. It must be noted however that the effect due to the diameter determined in the prior model remains identical and does not need to be redetermined. The three parameters which describe the effect of the diameter have been presented in Table 5.3. The resulting values for the new parameters of the thermodynamic property based semi-empirical model are given in Table 5.4.

TABLE 5.4 THERMODYNAMIC PROPERTY BASED SEMI-EMPIRICAL PARAMETERS

Parameter	Value	Parameter	Value	Parameter	Value
θ_T	0.3304	e	-1.2394	r	-0.9557
ω_T	1.8826	f	13.7338	s	1.3805
n_T	1.2685	g	-0.308	t	-0.3066
a	-26.2531	h	1.0391	u	-6.5604
b	2.92	i	2.7275	v	1.3399
c	-3.5323	j	0.9574	w	0.4983
d	18.1923	q	-1.0869	x	1.2795

With the parameters of the model determined, the spheroidization efficiency of the induction plasma process can be predicted for any of the powders as a function of the feed rate. It must be noted that the three initial parameters,θ_T,ω_T and n_T represent the effects of the plasma operating conditions. Once these are known for a system, the spheroidization efficiency of the powders can be determined. The resulting efficiency prediction for the set #7 through set #10 are presented in Figure 5.31. As it can be seen in Figure 5.31, the final model predicts the spheroidization efficiency accurately for all four different sets of powders. The only remaining variables which remain unknown in the model are the plasma operating conditions. Once an experimental set has been completed for particular operating conditions, the three main model parameters can be determined. Thereafter the complete system would be known for the wanted operating conditions.

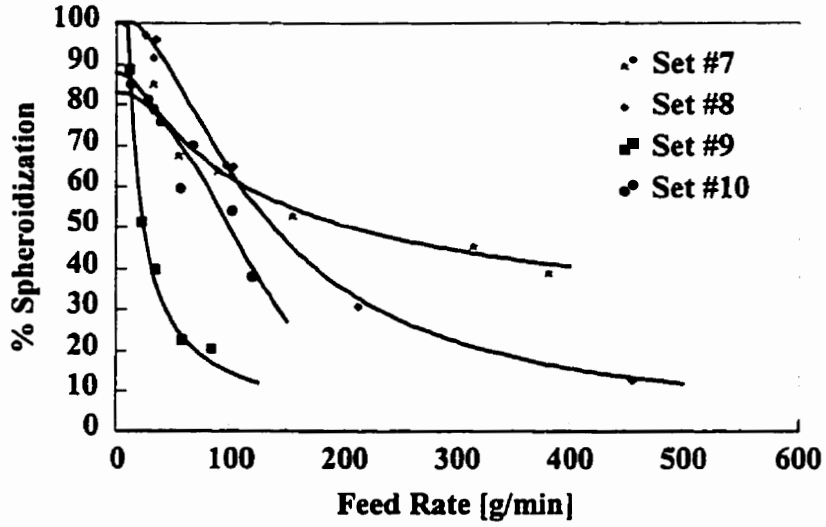

Figure 5.31 Spheroidization efficiency as predicted by the thermodynamic property based semi-empirical model for set #7 through set #10 which represents the silica, alumina, chromium oxide and zirconia powders

CHAPTER 6

SUMMARY AND CONCLUSIONS

An experimental study of the spheroidization of powders has been completed in order to obtain simple models. The purpose of obtaining these models is to obtain a method to predict the spheroidization efficiency of powder without having to require the use of extensive numerical simulations which also require that many assumptions be used. The use of the resulting models could be of importance in the industrial application of the induction plasma technology.

Initial analysis of the original and resulting powders have determine that assuming the absence of reactions between the particles and the plasma gases or simple phase change is possible if the plasma gases are chosen accordingly. The plasma gas environment should be chosen to avoid either the oxidation or the reduction of the powder. The phase changes which occur during the processing of the powders are also in accordance with the thermodynamic equilibrium diagram. The phases which are most stable at higher temperatures will be found in greater quantities in the resulting powders.

The other main assumption which was included in the study is that a minimum or a negligible amount of particle evaporation occurred. This was based on the fact that the optimum operating conditions are when the evaporation is minimized while most of the energy is used only for the melting. However, due to the wide variety of particle thermophysical properties, it was expected that some evaporation would occur. This resulted in smal energy efficiency fractions of the energy being used for unwanted phase changes.

It was also initially expected that the plasma treatment of the particles would have a densifying effect. The optical analyses of the powders revealed an opposite result. Due to the difference in density between the liquid and solid phases, the resulting powders contained cavities. The induction plasma processing melts the powders and eliminates any pores present prior to the processing. However, during the quenching phase, the larger liquid spheres solidify initially from the outward and consequently create cavities due to the subsequent shrinking of the particle core to its solid density. The rate of quenching and the thermodynamical properties of the powders would have to be taken into account to estimate the actual size of the cavities to be expected from the original powders.

The spheroidization efficiency of every experiment was obtained by image analysis. Significant differences were observe between the induction plasma installations and between the various powders. These results were used to analysis the theoretical, empirical and semi-empirical models suggested.

A theoretical approach which was based on the energy absorption capacity of the powder from the plasma was completed. The resulting model gave good results beyond the critical point except for a slight over estimation due to the eventual reduction in energy absorption efficiency. The critical point was defined as the instant when the maximum energy absorption efficiency by the powders is reached. The inconvenient of the model is that the preferred operating condition, which are at high spheroidization efficiency, are prior to the critical point.

The empirical model with the evaluated parameters gave very accurate predictions of the speroidization efficiency. The model is however useful only for the particular powder studied at the known plasma operating conditions.

The diameter based semi-empirical model expended the use of the earlier empirical model. The effect of the mean diameter of the powders was determined using experiments with identical plasma conditions and thermophysical properties while only varying the mean diameter of the particles. The resulting model did fulfill the wanted objective to determine the mean diameter effect on the model.

A final model was obtained by using a thermodynamic property based semi-empirical model. Since the effect of the diameter had been earlier determined, the only remaining varying parameter of the particles were the other key thermophysical properties. Experiments were therefore performed with identical plasma conditions and various powder to determine the parameters of the model. Even if the model can be considered complex, the predicted spheroidization efficiency for the silica, alumina, chromium oxide and zirconia powder correlated very accurately with the obtained experimental results.

The remaining unknown parameter which still have to be determined are a function of the plasma operating conditions. Two options are available, the first being to determine the three parameters for a variety of plasma operating conditions. Once a system has been evaluated, the model can be subsequently used. The second option would be to isolate some of the plasma operating conditions in a similar method as was used for the particles thermophysical properties.

However, as it was seen with the thermophysical properties, the model gets complicated quickly. For industrial application, the earlier case is the one favored since operating conditions for a process which has been optimized usually require minimal changes. The second option however can be used to estimate which parameters are of greater importance and which can be neglected.

6.1 Recommendations for Further Studies

Though all model were based on a macroscopic approach for the simplification of already available options, other phenomenons were proven to have great significance. It is the case for the microscopic study of the particles. As it was shown, the subsequent treatment of the powders by quenching is a key factor in controlling the quality of the powders. Many other properties of the powder should be taken into account in a microscopic approach as the variable density, the liquid phase surface tension, the diffusion of gases and other similar properties which all have been neglected and which also depend greatly on the temperature.

A progressive approach should be used such to eventually include more complex systems. An initially microscopic analysis of the melting and subsequent quenching of simple particles should be the logical first step. Thereafter, the introduction of other variables of interest as original particles formed from agglomerates could be done. Further studies could eventually even include the formation of spherical particles from multiphase clusters as is being used in the growing field of suspension plasma spraying (SPS).

REFERENCES

BOULOS, M.I., GAUVIN, W.H. (June 1974) *Powder Processing in a Plasma Jet*, The Canadian Journal of Chemical Engineering, Vol. 52, pp. 355-363.

BOULOS, M.I. (March 1976) *Flow and Temperture Fields in the Fire-Ball of an Inductively Coupled Plasma*, IEEE Transactions on Plasma Science, Vol. PS-4, No. 1, pp. 28-39.

BOULOS, M.I. (June 1978) *Heating of Powders in the Fire Ball of an Induction Plasma*, IEEE Transactions on Plasma Science, Vol. PS-6, No. 2, pp. 93-106.

BOULOS, M.I. (June 1991) *Advances in Induction Plasma Melting and Deposition of Materials*, 2nd Plasma - Technik Symposium, Lucerne, Switzerland, 16 pp.

BOULOS, M.I. (March 1992) *RF Induction Plasma Spraying: State-of-the-Art Review*, Journal of Thermal Spray Technology, Vol. 1, No. 1, pp. 33-40.

BOULOS, M.I., FAUCHAIS, P., PFENDER, E. (1994) *Thermal Plasmas Fundamentals and Applications Volume 1*, New-York, Plenum Press, 452 pp.

BOURDIN, E., FAUCHAIS, P., BOULOS, M.I. (1983) *Transient Heat Conduction under Plasma Conditions*, International Journal of Heat and Mass Transfer, Vol. 26, No. 4, pp. 567-582.

BOUYER, E., GITZHOFER, F., BOULOS, M.I. (February 1997a) *The Suspension Plasma Spraying of Bioceramics by Induction Plasma*, Journal of Materials, pp. 58-62.

BOUYER, E., GITZHOFER, F., BOULOS, M.I. (October 1997b) *Suspension Plasma Spraying for Hydroxyapatite Powder Preparation by RF Plasma*, IEEE Transactions on Plasma Science, Vol. 25, No. 5, pp. 1066-1072.

CLIFT, R., GRACE, J.R., WEBER, M.E. (1978) *Bubbles Drops and Particles*, New-York, Academic Press, 218 pp.

COULOMBE, S. (August 1994) *Diagnostic des particules en vol dans un plasma inductif*, Masters thesis, Université de Sherbrooke, Sherbrooke, 92 pp.

DIGNARD, N.M., BOULOS, M.I. (1997a) *Ceramic Powder Spheroidization under Induction Plasma Condition*, Proceedings of the 13th International Symposium on Plasma Chemistry, Beijing, China, August 1997, pp. 1031-1036.

DIGNARD, N.M., BOULOS, M.I. (1997b) *Ceramic and Metallic Powder Spheroidization using Induction Plasma Technology*, Proceedings of the United Thermal Spray Conference, Indianapolis, IN, USA, September 1997.

DIGNARD, N.M., BOULOS, M.I. (1998) *Metallic and Ceramic Powder Spheroidization by Induction Plasma*, Proceedings of the 15th International Thermal Spray Conference and Exhibition, Nice, France, May 1998.

ESSOLTANI, A., PROULX, P., BOULOS, M.I. (September 1990) *Radiation and Self-Absorption in Argon - Iron Plasmas at Atmospheric Pressure*, Journal of Analytical Atomic Spectrometry, Vol. 5, pp. 543-547.

ESSOLTANI, A., PROULX, P., BOULOS, M.I., GLEIZES, A. (February 1993) *A Combined Convective, Conductive and Radiative Heat Transfer Study for an Evaporating Metallic Particle under Plasma Conditions*, High Temperature Chemical Processes, Vol. 2, pp. 37-46.

ESSOLTANI, A., PROULX, P., BOULOS, M.I., GLEIZES, A. (1994) *Effect of the Presence of Iron Vapors on the Volumetric Emission of Ar/Fe and Ar/Fe/H_2 Plasmas*, Plasma Chemistry and Plasma Processing, Vol. 14, No. 3, pp. 301-315.

FAN, X (June 1994) *Induction Plasma Deposition of Alumina Free Standing Parts*, Ph.D. Thesis, Université de Sherbrooke, Sherbrooke, 171 pp.

FAUCHAIS, P. (1980) *Utilisation industrielle actuelle et potentielle des plasmas: synthèses, traitement des poudres, traitements métallurgiques, traitements de surface*, Revue de physique appliquée, Vol. 15, pp. 1281-1301.

GUO, J.Y., GITZHOFER, F., BOULOS, M.I. (1995) *Induction Plasma Synthesis of Ultrafine SiC Powders from Silicon and CH_4*, Journal of Material Science, Vol. 30, pp. 5589-5599.

ISHIGAKI, T., BOULOS, M.I. (1991) *In-Flight Ceramic Powder Treatment in an R.F. Induction Plasma*, Ceramic Transactions, Vol. 22, pp. 139-145.

JACQ, G., DURAND, J.P. (1992) *Situation économique de la projection thermique parmi les traitements et revêtements de surface*, Journal of High Temperature Chemical Processes, Vol. 1, Supplement to No. 3, pp. 57-75.

JIANG, X.L. (June 1994) *Induction Plasma Spraying of Refractory Materials*, Ph.D. Thesis, Université de Sherbrooke, Sherbrooke, 157 pp.

JIANG, X.L., GITZHOFER, F., BOULOS, M.I., TIWARI, R. (1995) *Reactive Deposotion of Tungsten and Titanium Carbides by Induction Plasma*, Journal of Material Science, Vol. 30, pp. 2325-2329.

KLIMA, R., KOTALIK, P. (September 1997) *On Cavities in Thermally Sphroidized Powder Particles*, Journal of Thermal Spray Technology, Vol. 6, No. 3, pp. 305-309.

MCKELLIGET, J.W. (1992) *A Mathematical Model of the Spheroidization of Porous Agglomerate Particles in Thermal Plasma Torches*, Thermal Plasma Applications in Materials and Metallurgical Processing, pp. 337-349.

MOSTAGHIMI, J., PROULX, P., BOULOS, M.I. (1985) *An Analysis of the Computer Modelling of the Flow and Temperature Fields in an Inductively Coupled Plasma*, Numerical Heat Transfer, Vol. 8, pp. 187-201.

MOSTAGHIMI, J., PROULX, P., BOULOS, M.I. (March 1987) *A Two-Temperature Model of the Inductively Coupled RF Plasma*, Journal of Applied Physics, Vol. 61, No. 5, pp. 1753-1760.

MOSTAGHIMI, J., BOULOS, M.I. (September 1990) *Effect of Frequency on Local Thermodynamic Equilibrium Conditions in an Inductively Coupled Argon Plasma at Atmospheric Pressure*, Journal of Applied Physics, Vol. 68, No. 6, pp. 2643-2648.

MUNZ, R.J. (1996) *Particulate Systems*, Course notes, McGill University, Montreal, 123 pp.

PAWLOWSKI, L. (1995) *The Science and Engineering of Thermal Spray Coatings*, West Sussex, England, John Wiley & Sons Ltd, 414 pp.

PFENDER, E., BOULOS, M.I., FAUCHAIS, P. (1985) *Methods and Principles of Plasma Generation*, Plasma Technology in Metallurgical Processing, pp. 27-47.

PFENDER, E. (1989) *Particle Behaviour in Thermal Plasmas*, Plasma Chemistry and Plasma Processing, Vol. 9, No. 1, supplementary, pp. 167-193.

POOLE, J.W., FREEMAN, M.P., DOAK, K.W., THORPE, M.L. (October 1973) *Simulator Tests to Study Hot-Flow Problems related to a Gas Core Reactor*, Washington, D.C., National Aeronautics and Space Administration, 113 pp.

PROULX, P., MOSTAGHIMI, J., BOULOS, M.I. (1985) *Plasma - Particle Interaction effects in Induction Plasma Modeling under Dense loading Conditions*, International Journal of Heat and Mass Transfer, Vol. 28, No. 7, pp. 1327-1336.

PROULX, P., MOSTAGHIMI, J., BOULOS, M.I. (1987) *Heating of Powders in an r.f. Inductively Coupled Plasma under Dense Loading Conditions*, Plasma Chemistry and Plasma Processing, Vol. 7, No. 1, pp. 29-52.

PROULX, P., BILODEAU, J.F. (1991a) *A Model for Ultrafine Powder Production in a Plasma Reactor*, Plasma Chemistry and plasma Processing, Vol. 11, No. 3, pp. 371-386.

PROULX, P., MOSTAGHIMI, J., BOULOS, M.I. (1991b) *Radiative Energy Transfer in Induction Plasma Modelling*, International Journal of Heat and Mass transfer, Vol. 34, No. 10, pp. 2571-2579.

REED, T.B. (1961) *Induction Coupled Plasma Torch*, Journal of Applied Physics, Vol. 32, pp. 821-824.

SCHEIBEL, E.G. (1954) *Liquid Diffusivities*, Industrial and Engineering Chemistry, Correspondence, Vol. 46, No. 9, pp. 2007-2008.

VARDELLE, M., VARDELLE, A., FAUCHAIS, P., TRASSY, C., PROULX, P. (1990) *Experimental and Numerical Investigation of Powder Vaporization under Thermal Plasma Conditions*, Colloque de physique, Colloque C5, supplément au n°18, Tome 51, pp. C5(171-179).

WILKE, C.R. (1949) *Estimation of Liquid Diffusion Coefficients*, Chemical Engineering Progress, Vol. 45, No. 3, pp. 218-224.

YOSHIDA, T., TANI, T., NISHIMURA, H., AKASHI, K. (1983) *Characterization of a Hybrid Plasma and its Application to a Chemical Synthesis*, Journal of Applied Physics, Vol. 54, No. 2, pp. 640-646.